Tetrahedral, Highly Coordinatively Unsaturated 14e (Fe) and 15e (Co) Hydrocarbyl Complexes Bearing Hydrotris(pyrazolyl)borato Ligands ($Tp^{R'}$), $Tp^{R'}M-R$ (M = Fe, Co, Ni)

Nobuhiko Shirasawa, Trieu Thi Nguyet,[1] Shiro Hikichi, Yoshihiko Moro-oka, and Munetaka Akita*

Chemical Resources Laboratory, Tokyo Institute of Technology, 4259 Nagatsuta, Midori-ku, Yokohama 226-8503, Japan

Received April 17, 2001

A series of hydrocarbyl complexes supported only by hydrotris(pyrazolyl)borato ligands ($Tp^{R'}$ = 3,5-diisopropylpyrazolyl (Tp^{iPr2}) and 3,4,5-trimethylpyrazolyl derivatives (Tp^{Me3})), $Tp^{R'}M-R$ (M/R/R′ = Ni/η^3-allyl/iPr_2 (**2^{iPr2}Ni**), Co/η^3-allyl/iPr_2 (**2^{iPr2}Co**), Fe/η^1-allyl/iPr_2 (**2^{iPr2}Fe**), Ni/η^3-prenyl/iPr_2 (**3^{iPr2}Ni**), Co/η^1-*p*-methylbenzyl/iPr_2 (**4^{iPr2}Co**), Fe/η^1-*p*-methylbenzyl/iPr_2 (**4^{iPr2}Fe**), Co/η^1-*p*-methylbenzyl/Me_3 (**4^{Me3}Co**), Fe/η^1-*p*-methylbenzyl/Me_3 (**4^{Me3}Fe**), Co/η^1-α-naphthylmethyl/iPr_2 (**5^{iPr2}Co**), Co/η^1-ethyl/iPr_2 (**6^{iPr2}Co**), Fe/η^1-ethyl/iPr_2 (**6^{iPr2}Fe**)) is prepared by reaction of the corresponding precursors, $Tp^{iPr2}M-Cl$ (M = Fe (**1^{iPr2}Fe**), Co (**1^{iPr2}Co**), Ni (**1^{iPr2}Ni**)) or $Tp^{Me3}M(\kappa^2\text{-X})$ (M/X = Co/NO_3 (**1′^{Me3}Co**), Fe/OAc (**1′^{Me3}Fe**)), with appropriate Grignard reagents. η^1-Hydrocarbyl complexes are obtained when M = Fe, Co, and the thermally unstable η^1-ethylnickel derivative **6^{iPr2}Ni** is characterized via conversion to the acyl derivative $Tp^{iPr2}Ni(CO)C(=O)Et$ (**12**). Characterization by a combination of various spectroscopic methods (IR, NMR, UV, and ESR), magnetic susceptibility, X-ray crystallography, and chemical reactions reveals that the η^1-hydrocarbyl complexes **2^{iPr2}Fe** and **4**−**6** are tetrahedral, highly coordinatively unsaturated species with 14 (M = Fe) and 15 (M = Co) valence electrons. It is remarkable that the ethyl complexes **6** are thermally stable even at higher temperatures (70 °C (Co); 110 °C (Fe)), although they contain β-hydrogen atoms. The presence of a metal−carbon bond in **4**−**6** has been confirmed by protonation and hydrogenolysis, giving alkane (R−H) and carbonylation leading to acyl−carbonyl species ($Tp^{R'}M(CO)_nC(=O)R$: M/*n* = Fe/2 (**7**), Co/1 (**8**)). Despite the coordinative unsaturation at the metal centers complexes **4**−**6** turn out to be sluggish toward unsaturated organic compounds such as olefin, internal acetylene, ketone, and nitrile. Only phenylacetylene reacted with the ethyl complexes **6^{iPr2}** to result in insertion of the C≡C bond into the M−C bond (**6^{iPr2}Co**) or protonolysis of the M−C bond to afford the acetylide complex $Tp^{iPr2}FeC{\equiv}CPh$, which was characterized after carbonylation, giving $Tp^{iPr2}Fe(CO)_2C{\equiv}CPh$ (**12**). The magnetic susceptibility of η^1-hydrocarbyl complexes combined with the results of EHMO calculations for the model complexes $Tp^{H}M-CH_3$ (M = Fe, Co) reveals the high-spin configuration of d electrons, which leads to occupation of all five frontier orbitals by electron pairs or unpaired electrons. The lack of a vacant d orbital is concluded to be the origin of the thermal stability of the electron-deficient hydrocarbyl complexes.

Introduction

Coordinatively unsaturated hydrocarbyl complexes are key intermediates of stoichiometric and catalytic C−C coupling reactions mediated by organometallic species such as olefin polymerization,[2] and it is essential to accumulate information on their structure and reactivity for improvement of the efficiency of the transformations and development of new reactions.

Although 16-valence-electron species such as square-planar d^8 metal complexes and early-transition-metal complexes have been studied extensively,[2] very few examples of *late-transition-metal hydrocarbyl complexes with less than 16 valence electrons* have been reported so far. Some typical previous examples are shown in Chart 1.[3−7] As can be seen from the structures, almost all the previous examples contain bulky hydrocarbyl ligands without β-hydrogen atoms, such as ortho-disubstituted aryl groups (**I**, **II**) and $CH_2ER'_3$ groups (**IV**−**VII**: E = C, Si), which can kinetically stabilize the

(1) A UNESCO fellow (1997−1998) on leave from the Department of Chemistry, Hanoi National University.

(2) Yamamoto, A. *Organotransition Metal Chemistry*; Wiley-Interscience: New York, 1986. Collman, J. P.; Hegedus, L. S.; Norton, J. R.; Finke, R. G. *Principles and Applications of Organotransition Metal Chemistry*, 2nd ed.; University Science Books: Mill Valley, CA, 1987. Crabtree, R. H. *The Organometallic Chemistry of the Transition Metals*, 3rd ed.; Wiley-Interscience: New York, 2001. Cornils, B.; Herrmann, W.; *Applied Homogeneous Catalysis with Organometallic Compounds*; VCH: Oxford, U.K., 1996. Abel, E. W.; Stone, F. G. A.; Wilkinson, G. *Comprehensive Organometallic Chemistry II*; Pergamon: Oxford, U.K., 1995.

10.1021/om0103106 CCC: $20.00
Publication on Web 07/13/2001

Chart 1

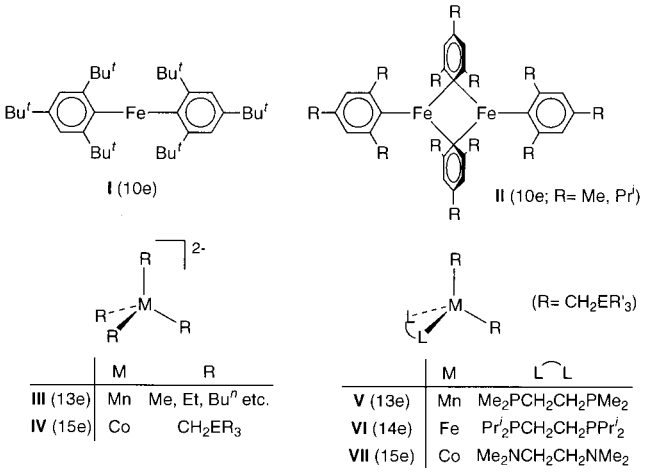

	M	R
III (13e)	Mn	Me, Et, Bu^n etc.
IV (15e)	Co	CH_2ER_3

	M	L⌒L
V (13e)	Mn	$Me_2PCH_2CH_2PMe_2$
VI (14e)	Fe	$Pr^i_2PCH_2CH_2PPr^i_2$
VII (15e)	Co	$Me_2NCH_2CH_2NMe_2$

Scheme 1

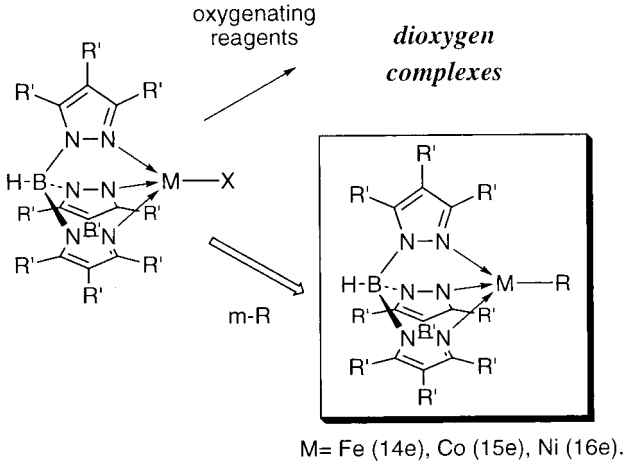

coordinatively unsaturated species by shielding the metal centers. The anionic homoleptic manganese complexes **III** reported by Girolami et al. are the only complexes which contain hydrocarbyl groups bearing β-hydrogen atoms,[3b] but X-ray crystallography of the ethyl derivative reveals the additional interaction of the α-carbons of the ethyl groups with the countercation (Li), which may contribute to stabilization of such a structure.

The systematic synthetic study of dioxygen complexes bearing hydrotris(pyrazolyl)borato ligands (Tp$^{R'}$)[8,9] has been one of the targets of our recent research activity.[10] The Tp$^{R'}$ ligand is recognized as a "tetrahedral enforcer", and a variety of dioxygen complexes have been prepared by treatment of tetrahedral Tp$^{R'}$M−X type precursors with oxygenating reagents. If such precursors could be alkylated, we would be able to have an opportunity to study the chemistry of tetrahedral, highly coordinatively unsaturated organometallic species with less than 16 valence electrons when M = Fe, Co (Scheme 1).

Herein we disclose full details of the results of the study on Tp$^{R'}$M−R-type coordinatively unsaturated hydrocarbyl complexes. Part of the results have already been reported in two communications,[11] which were followed by two closely related reports on PhTp^{tBu}Fe−Me and Tp^{tBu,Me}Co−R by Parkin and Theopold (see Chart 3),[6] respectively, indicating increasing attention to this research area.

Results and Discussion

Synthesis and Characterization of Allyl Complexes 2^{iPr2}. The first attempts that we made were syntheses of allyl complexes, because the allyl ligand was anticipated to stabilize electron-deficient metal centers through η^3-coordination working as a 4e donor.[2]

Treatment of chloro complexes of iron, cobalt, and nickel (**1^{iPr2}**) with allylmagnesium chloride in THF followed by extraction with pentane and crystallization

(3) (a) Howard, C. G.; Girolami, G. S.; Wilkinson, G.; Thornton-Pett, M.; Hursthouse, M. B. *J. Chem. Soc., Dalton Trans.* **1983**, 2631. (b) Morris, R. J.; Gilorami, G. S. *Organometallics* **1989**, *8*, 1478. (c) Buttrus, N. H.; Eaborn, C.; Hitchcock, P. B.; Smith, J. D.; Sullivan, A. C. *J. Chem. Soc., Chem. Commun.* **1985**, 1380. (d) Wehmschulte, R.; Power, P. P. *Organometallics* **1995**, *14*, 3264. (e) Hursthouse, M. B.; Izod, K. J.; Motevalli, M.; Thornton, P. *Polyhedron* **1996**, *15*, 135.

(4) (a) Chatt, J.; Shaw, B. L. *J. Chem. Soc.* **1961,** 285. (b) Hermes, A. R.; Girolami, G. S. *Organometallics* **1987,** *6,* 763. (c) Müller, H.; Seidel, W.; Görls, H. *J. Organomet. Chem.* **1992**, *445*, 133. (d) Klose, A.; Solari, E.; Floriani, C.; Chiesi-Villa, A.; Rizzoli, C.; Re, N. *J. Am. Chem. Soc.* **1994**, *116*, 9123. (e) Müller, H.; Seidel, W.; Görls, H. *Angew. Chem., Int. Ed. Engl.* **1995**, *34*, 325. (f) Leung, W.-P.; Lee, H. K.; Weng, L.-H.; Luo, B.-S.; Zhou, Z.-Y.; Mak, T. W. C. *Organometallics* **1996**, *15*, 1785. (g) Fryzuk, M. D.; Leznoff, D. B.; Ma, E. S. F.; Rettig, S. J.; Young, V. G., Jr. *Organometallics* **1998**, *17*, 2313.

(5) (a) Theopold, K. H.; Silvestre, J.; Byrne, E. K.; Richeson, D. S. *Organometallics* **1989**, *8*, 2001. (b) Hay-Motherwell, R. S.; Wilkinson, G.; Hussain, B.; Hursthouse, M. B. *Polyhedron* **1990**, *9*, 931. (c) Hursthouse, M. B.; Izod, K. J.; Motevalli, M. Thornton, P. *Polyhedron* **1996**, *15*, 135. (d) Fryzuk, M. D.; Leznoff, D. B.; Thompson, R. C.; Rettig, S. J. *J. Am. Chem. Soc.* **1998**, *120*, 10126.

(6) (a) Kisko, J. L.; Hascall, T.; Parkin, G. *J. Am. Chem. Soc.* **1998**, *120*, 10561. (b) Jewson, J. D.; Liable-Sands, L. M.; Yap, G. P. A.; Rheingold, A. L.; Theopold, K. H. *Organometallics* **1999**, *18*, 300. See also a recent related paper: (c) Schebler, P. J.; Mandimutsira, B. S.; Riordan, C. G.; Liable-Sands, L. M.; Incarvito, C. D.; Rheingold, A. L. *J. Am. Chem. Soc.* **2001**, *123*, 331.

(7) Huang, D.; Streib, W. E.; Bollinger, C. J.; Caulton, K. G.; Winter, R. F.; Scheiring, T. *J. Am. Chem. Soc.* **1999**, *121*, 8087.

(8) Abbreviations used in this paper: Tp$^{R'}$, hydrotris(pyrazolyl)-borato ligands; Tp^{iPr2}, 3,5-diisopropylpyrazolyl derivative; Tp^{Me3}, 3,4,5-trimethylpyrazolyl derivative; Tp^{H}, the nonsubstituted parent ligand; pz$^{R'}$, pyrazolyl group in Tp$^{R'}$; 4-pz-H, the hydrogen atom at the 4-position of pz$^{R'}$; 3-, 4-, and 5-pz: the pz ring carbon atoms at 3-, 4-, and 5-positions, respectively. The compound number, superscript, and element denote the hydrocarbyl ligand, the Tp$^{R'}$ ligand, and the central metal, respectively. For example, the Tp^{iPr2}Fe-*p*-methylbenzyl complex is abbreviated as **4^{iPr2}Fe**, where **4**, **iPr2**, and **Fe** denote the *p*-methylbenzyl ligand, the Tp^{iPr2} ligand, and the central iron metal, respectively.

(9) Trofimenko, S. *Scorpionates: The Coordination Chemistry of Polypyrazolylborate Ligands*; Imperial College Press: London, England, 1999.

(10) Our recent works on Tp$^{R'}$M−O$_2$ complexes are as follows. Ni, Co: (a) Hikichi, S.; Komatsuzaki, H.; Akita, M.; Moro-oka, Y. *J. Am. Chem. Soc.* **1998**, *120*, 4699. (b) Hikichi, S.; Yoshizawa, M.; Sasakura, Y.; Akita, M.; Moro-oka, Y. *J. Am. Chem. Soc.* **1998**, *120*, 10567. (c) Hikichi, S.; Yoshizawa, M.; Sasakura, Y.; Komatsuzaki, H.; Akita, M.; Moro-oka, Y. *Chem. Lett.* **1999**, 979. Rh: (d) Akita, M.; Ohta, K.; Takahashi, Y.; Hikichi, S.; Moro-oka, Y. *Organometallics* **1997**, *16*, 4121. (e) Takahashi, Y.; Hashimoto, M.; Hikichi, S.; Akita, M.; Moro-oka, Y. *Angew. Chem., Int. Ed.* **1999**, *38*, 3074. (f) Akita, M.; Hashimoto, M.; Hikichi, S.; Moro-oka, Y. *Organometallics* **2000**, *19*, 3744. Ru: (g) Takahashi, Y.; Akita, M.; Hikichi, S.; Moro-oka, Y. *Organometallics* **1998**, *17*, 4884. (h) Takahashi, Y.; Hikichi, S.; Akita, M.; Moro-oka, Y. *J. Chem. Soc., Chem. Commun.* **1999**, 1491. Pd: (i) Akita, M.; Miyaji, T.; Hikichi, S.; Moro-oka, Y. *J. Chem. Soc., Chem. Commun.* **1998**, 1005. (j) Akita, M.; Miyaji, T.; Hikichi, S.; Moro-oka, Y. *Chem. Lett.* **1999**, 813. V: (k) Kosugi, M.; Hikichi, S.; Akita, M.; Moro-oka, Y. *J. Chem. Soc., Dalton Trans.* **1999**, 1369. Review: (l) Akita, M.; Hikichi, S.; Moro-oka, Y. *J. Synth. Org. Chem.* **1999**, *57*, 619 (in Japanese). (m) Hikichi, S.; Akita, M.; Moro-oka, Y. *Coord. Chem. Rev.* **2000**, *198*, 61.

(11) (a) Akita, M.; Shirasawa, N.; Hikichi, S.; Moro-oka, Y. *J. Chem. Soc., Chem. Commun.* **1998**, 973. (b) Shirasawa, N.; Akita, M.; Hikichi, S.: Moro-oka. Y. *J. Chem. Soc., Chem. Commun.* **1999**, 417.

at a low temperature afforded yellow (**2^{iPr2}Fe**), dark orange (**2^{iPr2}Co**), and deep red crystals (**2^{iPr2}Ni**) (eq 1).

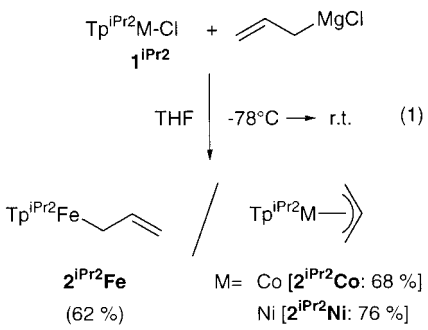

In contrast to the stable diamagnetic Ni complex **2^{iPr2}Ni**, the other two paramagnetic products **2^{iPr2}Fe,Co** were sensitive to moisture and the air. Reaction of the manganese complex **1^{iPr2}Mn** resulted in disproportionation to give the sandwich complex Mn(κ^3-Tp^{iPr2})$_2$.[12]

The diamagnetic Ni complex **2^{iPr2}Ni** was first characterized by spectroscopic methods. The η^3-coordination of the allyl ligand is indicated by the three ^{1}H NMR allyl signals (δ_H (C_6D_6) 6.15−5.85 (1H, m, central CH), 3.23 (2H, d, J = 6.7 Hz, *syn*-CH_2), 2.42 (2H, d, 12.3 Hz, *anti*-CH_2)) typical for such a coordination mode. As for the pz^{iPr2} signals, observation of only one set of the averaged signals suggests occurrence of a dynamic behavior, which was not frozen out even at −80 °C (when observed at 270 MHz). The mechanism of the dynamic behavior should involve pseudorotation of the Tp^{iPr2} ligand associated with κ^2−κ^3 interconversion.[13] Taking into account the ν_{BH} vibration at 2531 cm^{-1} (KBr) indicating κ^3-coordination of the Tp^{iPr2} ligand,[10d] the results of the spectroscopic analyses and the diamagnetism lead to the conclusion that structure of the nickel complex **2^{iPr2}Ni** is described as a low-spin, square-pyramidal complex with the η^3-allyl and κ^3-Tp^{iPr2} ligands, which is confirmed by X-ray crystallography.

An ORTEP view and selected structural parameters of **2^{iPr2}Ni** are shown in Figure 1 and Table 1, respectively. In accord with the spectroscopic characterization, **2^{iPr2}Ni** adopts a square-pyramidal geometry with the C1−C3−N11−N21 basal plane, as indicated by the Σ value (the sum of inter-basal ligand angles: ∼360°), and the nickel atom is located slightly above the basal plane (Δ_1). The *supine*-allyl ligand[14] is almost symmetrically bonded to the nickel center with Ni−C separations of ca. 2.0 Å. The Tp^{iPr2} ligand is also coordinated to the nickel center in a mirror-symmetrical manner, judging from the similar Ni−N11 (1.962(6) Å) and −N21 distances (1.962(5) Å) and the very small differences in the ∠N31−Ni−N(basal) (Δ_2) and ∠N31−Ni−C(1,3) angles (Δ_3). The axial nitrogen atom (N31) is located ca. 0.25 Å further away from the metal center than the other two basal nitrogen atoms (N11 and N21). The weak coordination of N31 should be related to the dynamic behavior mentioned above, and the ν_{BH} vibration (2471 cm^{-1}) observed in a hexane solution indicates conversion to a κ^2-Tp^{iPr2} species in a solution.[10d] The allyl ligand is slightly tilted away from a perpendicular arrangement, as is evident from the dihedral angle between the allyl ligand mean plane and the basal plane (θ_1). This is due to the steric repulsion with the Tp^{iPr2} ligand, because the allyl ligands in a less hindered complex (e.g., Ni(η^3-allyl)$_2$)[15] are tilted toward the opposite direction. The spectroscopic and structural features of **2^{iPr2}Ni** were very similar to those of a related compound with the nonsubstituted ligand, Tp^{H}Ni(η^3-allyl), reported by Lehmkuhl.[16]

The cobalt complex **2^{iPr2}Co** is characterized by ^{1}H NMR, IR, UV, magnetic susceptibility, and X-ray crystallography. The isotropically shifted ^{1}H NMR spectrum[17] containing the averaged pz^{iPr2} signals (allyl signals not located) and the ν_{BH} vibration (KBr; 2536 cm^{-1})[10d] indicates fluxional properties and κ^3-coordination of the Tp^{iPr2} ligand, respectively, and the averaged ^{1}H NMR signals for the Tp^{iPr2} moiety should be interpreted in terms of a mechanism similar to that of the nickel complex **2^{iPr2}Ni**. In general, tetrahedral Tp$^{R'}$Co−X species show d−d transitions of ϵ >300 in the range of 500−600 nm (Figure 2b; cf. **6^{iPr2}Co**; for details, see below), but an UV−vis spectrum of the dark orange **2^{iPr2}Co** contains a very weak absorption at 647 nm (ϵ 40; Figure 2a), suggesting that the allyl complex is not a tetrahedral species. The effective magnetic moment (μ_{eff}) of **2^{iPr2}Co** determined to be 1.8 μ_B (S = $^1/_2$) indicates the presence of one unpaired electron, which is consistent with a low-spin configuration resulting from a square-planar or square-pyramidal geometry.[18] These results are consistent with a five-coordinate, square-pyramidal geometry similar to that of the nickel complex, which is also confirmed by X-ray crystallography (Figure 1). Molecular structures and structural parameters (Table 1) of the nickel and cobalt complexes are similar. The difference between the M−N$_{ax}$ and M−N$_{eq}$ distances becomes smaller than that of the Ni complex (0.16 Å for Co vs 0.24 Å for Ni), indicating that, in the Co complex, the axial ligand is more tightly bound to the metal center due to an increase of Lewis acidity of the metal center with a smaller number of d electrons (d^7 (Co) vs d^8 (Ni)). In accord with this observation, the κ^3 form is retained even in solution, judging from the ν_{BH} vibration of a hexane solution (2536 cm^{-1}).

In sharp contrast to the low-spin Ni and Co complexes, the iron complex **2^{iPr2}Fe** turns out to be a high-spin species, as revealed by the magnetic susceptibility (μ_{eff} = 5.0 μ_B; S = 2). This electronic configuration suggests a tetrahedral geometry, which was also consistent with the NMR (one set of the averaged pz^{iPr2} signals) and IR data (ν_{BH} 2543 cm^{-1}).[10d] No valuable information is obtained by UV−vis spectroscopy, be-

(12) Mn(Tp^{iPr2})$_2$ was characterized by preliminary X-ray crystallography. Cell parameters: a = 28.188(8) Å, b = 12.263(5) Å, c = 21.54-(1) Å, β = 112.43(2)°, V = 6883(5) Å^3.

(13) See refs 10d,f,g and references therein.

(14) Yasuda, H.; Tatsumi, K.; Okamoto, T.; Mashima, K.; Lee, K.; Nakamura, A.; Kai, Y.; Kanehisa, N.; Kasai, N. *J. Am. Chem. Soc.* **1985**, *107*, 2410.

(15) Goddard, R.; Krüger, C.; Mark, F.; Stansfield, R.; Zheng, X. *Organometallics* **1985**, *4*, 285.

(16) Lehmkuhl, H.; Näser, J.; Mehler, G.; Keil, T.; Danowski, F.; Benn, R.; Mynott, R.; Schroth, G.; Gabor, B.; Krüger, C.; Betz, P. *Chem. Ber.* **1991**, *124*, 441.

(17) (a) La Mar, G. N.; Horrocks, W. D. W., Jr.; Holm, R. H. *NMR of Paramagnetic Molecules: Principles and Applications*; Academic Press: New York, 1973. (b) Lever; A. B. P. *Coord. Chem. Rev.* **1996**, *150*, 1−292.

(18) (a) Shriver, D. F.; Atkins, P. W. *Inorganic Chemistry*, 3rd ed.; Oxford University Press: Oxford, U.K., 1999. (b) Cotton, F. A.; Wilkinson, G.; Murillo, C. A.; Bochmann, M. *Advanced Inorganic Chemistry*, 6th ed.; Wiley-Interscience: New York, 1999.

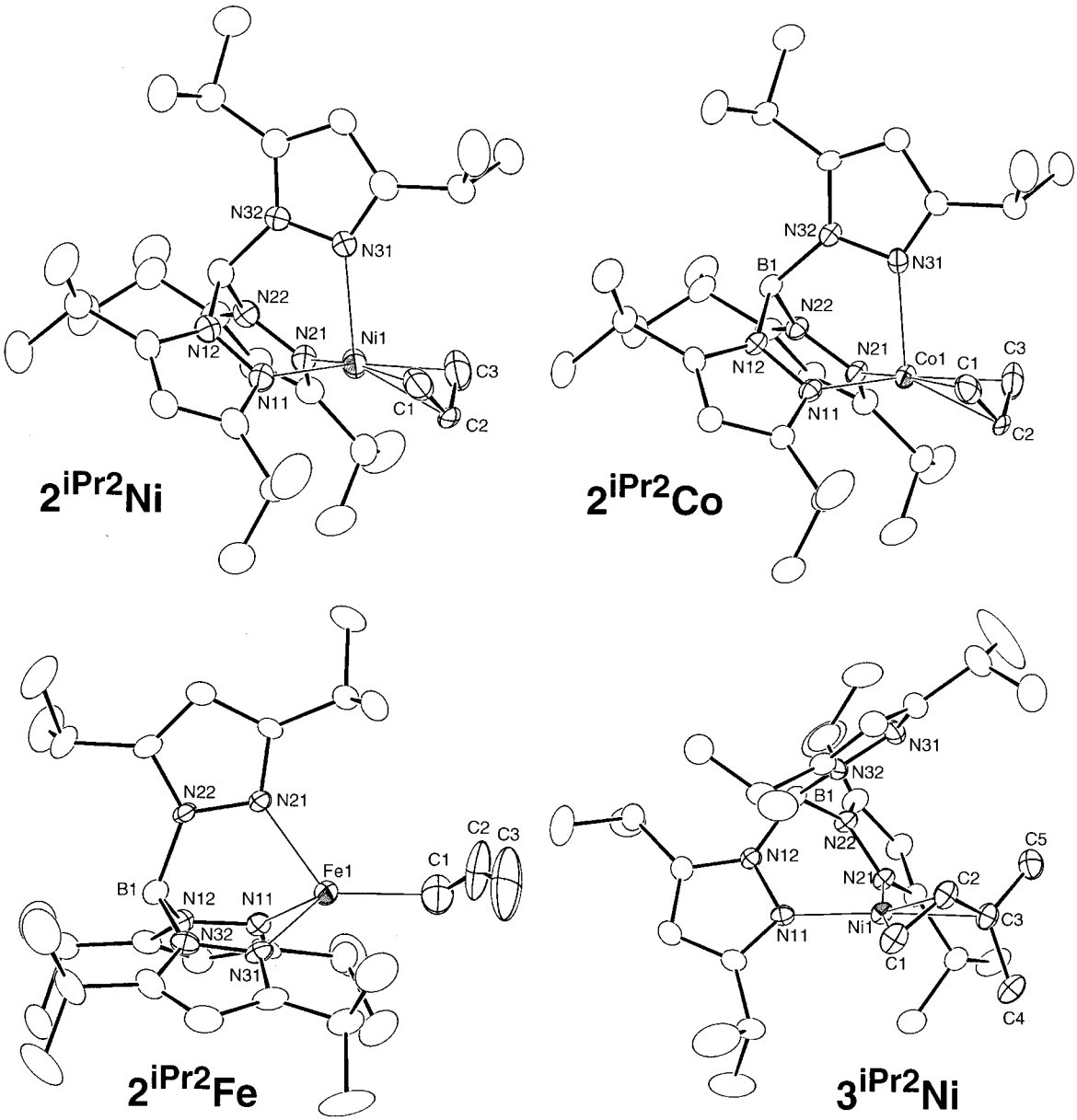

Figure 1. Molecular structures of $Tp^{iPr2}M-$allyl complexes drawn at the 30% probability level.

cause Fe(II) species usually do not show any characteristic absorption. The tetrahedral geometry was verified by X-ray crystallography. Two independent molecules with essentially the same geometry are included in a unit cell, and an ORTEP view of one of them is shown in Figure 1. Their structural parameters are summarized in Table 1. As is evident from the molecular structure, the distances from C2 (~2.9 Å) and C3 atoms (~3.7 Å) to the iron center are far beyond the range of bonding interactions (~2 Å), indicating η^1-coordination of the allyl ligand. In contrast to the square-pyramidal complexes **2^{iPr2}Ni,Co**, the three coordinated nitrogen atoms in the tetrahedral complex **2^{iPr2}Fe** are located almost equidistant from the Fe center (~2.1 Å) and the C1−Fe−N angles are in a narrow range (119−130°).

It is remarkable that, although the iron atom contains a smaller number of d electrons (d^6, Fe(II)) compared to the other two counterparts (d^7, Co(II); d^8, Ni(II)), the resulting allyl complex adopts a η^1 structure with 14e configuration rather than a η^3 structure with 16e configuration closer to the coordinatively saturated electronic configuration (18e) as observed for the Ni (18e) and Co systems (17e) (Chart 2).We also attempted preparation of a (η^1-allyl)nickel complex by introduction of substituents at one of the two allyl terminal carbon atoms. We expected that the steric repulsion between the alkyl substituents and the Tp^{iPr2} ligand might give rise to change of the coordination mode of the allyl ligand from η^3 to η^1. The prenyl complex **3^{iPr}Ni**, bearing two geminal methyl groups at the allyl terminus, was prepared by the Grignard method (eq 2).

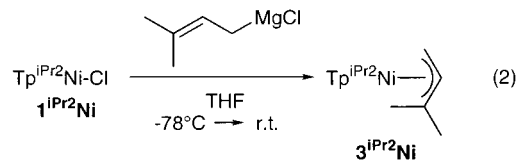

(2)

In contrast to our expectation, the product is diamagnetic and a ^{1}H NMR spectrum observed at room temperature reveals occurrence of dynamic behavior of not

Table 1. Selected Structural Parameters for Allyl Complexes 2^{iPr2} and $3^{iPr2}Ni$

			$2^{iPr2}Fe$[a]		
	$2^{iPr2}Ni$	$2^{iPr2}Co$	molec 1 (a series)	molec 2 (b series)	$3^{iPr2}Ni$
Interatomic Distances (Å)					
C1−C2	1.45(1)	1.484(9)	1.29(2)	1.40(2)	1.409(4)
C2−C3	1.33(1)	1.375(8)	1.24(3)	1.15(3)	1.406(4)
M−C1	1.995(8)	2.068(6)	2.03(1)	2.10(1)	2.011(3)
M−C2	2.034(5)	2.055(4)	2.87(1)	2.93(1)	1.953(2)
M−C3	2.00(1)	2.075(7)	3.74(2)	3.78(2)	2.103(2)
M−N11	1.962(6)	1.985(4)	2.076(6)	2.091(6)	1.934(2)
M−N21	1.969(5)	1.996(4)	2.079(7)	2.091(7)	1.944(2)
M−N31	2.220(5)	2.152(4)	2.094(8)	2.070(8)	3.560(2)
Bond Angles (deg)					
C1−M−C3	71.1(4)	71.5(3)			72.3(1)
C1−M−N11	97.3(3)	97.0(2)	119.1(4)	119.5(3)	98.49(9)
C1−M−N21	167.9(4)	171.4(2)	127.1(5)	131.6(4)	170.31(8)
C1−M−N31	98.8(3)	93.7(2)	130.5(5)	125.7(4)	
C3−M−N11	165.3(3)	165.9(2)			170.73(9)
C3−M−N21	100.3(3)	101.1(2)			99.56(8)
C3−M−N31	99.6(3)	96.6(2)			
N11−M−N21	89.7(2)	89.6(2)	89.5(3)	89.9(3)	89.71(7)
N11−M−N31	90.9(2)	92.2(2)	89.3(3)	90.1(3)	
N21−M−N31	90.9(2)	91.5(2)	89.3(3)	88.3(3)	
Calculated Parameters					
Σ[b]	358.9	357.3			360.1
Δ_1[c]	0.17 [d]	0.12 [d]			0.04[e]
Δ_2[f]	0	0.7			0.07[g]
Δ_3[h]	0.8	2.9			4.89[i]
θ_1[j]	81.5	80.3			80.0

[a] A unit cell contains two independent molecules. [b] Sum of ∠C1-M−C3, ∠C1−M−N11, ∠C3−M−N21, and ∠N11−M−N21 (in deg). [c] Distance between M and the mean plane C1−C3−N11−N21 (in Å). [d] Above the plane. [e] Below the plane. [f] |∠N11−M−N31 − ∠N21−M−N31| (in deg). [g] |∠N111−Ni1−B1 − ∠N21−Ni1−B1| (in deg). [h] |∠C1−M−N31 − ∠C3−M−N31| (in deg). [i] |∠C1−Ni1−B1 − ∠C3−Ni1−B1| (in deg). [j] Dihedral angles between planes M−N11−N21 and C1−C2−C3 (in deg).

only the Tp^{iPr2} ligand (a single set of the pz^{iPr2} signals) as observed for **2^{iPr}Ni** but also the prenyl ligand. The spectrum observed at −30 °C contains the prenyl signals consistent with a η^3 coordination but, when the temperature is raised to 70 °C, the prenyl CH_2 signals are coalesced into a broad single resonance and the CH signal changes to a triplet signal.

The molecular structure of **3^{iPr2}Ni** determined by X-ray crystallography is shown in Figure 1, and selected structural parameters are listed in Table 1. The prenyl complex adopts a four-coordinate, square-planar geometry, which is different from the five-coordinate, square-pyramidal geometry of the allyl complex **2^{iPr2}Ni**, as is evident from (1) the κ^2-coordination of the Tp^{iPr2} ligand and (2) *prone* arrangement[14] of the prenyl ligand with respect to the Tp^{iPr2}Ni backbone. However, the structural parameters associated with the N_2NiC_2 moiety are essentially the same as those of **2^{iPr2}Ni**, although (1) the coordination to the Ni center becomes unsymmetrical to a small extent (cf. $|d(Ni1-C1) - d(Ni1-C3)| = 0.092$ Å (cf. **2^{iPr2}Ni**: ∼0 Å)) and (2) the Δ_3 value indicates slight twisting of the prenyl ligand with respect to the Ni−prenyl axis. These structural changes should result mainly from the steric repulsion between the bulky Tp^{iPr2} and dimethyl-substituted allyl ligands, and the steric congestion brought about by the prenyl ligand is released by deformation to a κ^2-Tp^{iPr2} species rather than to a η^1-prenyl structure. In accord with the X-ray structure, the Tp^{iPr2} ligand is coordinated to the Ni center in a κ^2 fashion even in solution, as judged by the ν_{BH} vibration (2472 cm^{-1}).[10d] Thus, the introduction of the bulky prenyl ligand does not change the prenyl coordination mode but the Tp^{iPr2} coordination mode from κ^3 to κ^2 to give the square-planar complex.

Taking into account the solid-state structure, the complicated dynamic NMR behavior would be interpreted in terms of a combination of (a) $\eta^3-\eta^1$ interconversion, (b) rotation, (c) flipping of the allyl ligand, and (d) pseudorotation of the Tp^{iPr2} ligand associated with $\kappa^2-\kappa^3$ interconversion.[13] The spectral features at a higher temperature are *apparently* consistent with a C_{3v} symmetrical structure. It is concluded, however, that a tetrahedral C_{3v}-symmetrical species as observed for the iron derivative **2^{iPr2}Fe** is not an intermediate of the dynamic behavior, because all processes can be followed by ^1H NMR and a tetrahedral high-spin species should be paramagnetic.

Thus, allylation of **1^{iPr2}** affords the low-spin square-pyramidal species (Co and Ni), when the allyl ligand is regarded as a 4e donor occupying two coordination sites, and the high-spin tetrahedral species (Fe). In particular, the formation of the latter product, which was a desired highly electron-deficient 14e species with tetrahedral geometry, encouraged us to further examine synthesis of related hydrocarbyl complexes.

Synthesis of η^1-Hydrocarbyl Complexes. Our efforts were then directed to synthesis of benzyl type complexes which did not contain β-hydrogen atoms (Scheme 2). The *p*-methylbenzyl derivatives of iron (pale yellow) and cobalt (deep green), $Tp^{iPr2}M-CH_2C_6H_4$-*p*-Me (**4^{iPr2}Fe,Co**), were successfully prepared by the Grignard method similar to the synthesis of the allyl complexes **2^{iPr2}**. However, reaction of the nickel complex **1^{iPr2}Ni** with various Grignard reagents resulted in decomposition to give a mixture of products, from which no characterizable product was isolated, although the trapping experiment with CO revealed formation of the corresponding thermally unstable hydrocarbyl complexes, as will be described below. Because a single crystal of the cobalt derivative **4^{iPr2}Co** could not be obtained, structural analysis was performed for the α-naphthylmethyl derivative **5^{iPr2}Co**.

To examine the steric shielding effect by the bulky Tp^{iPr2} ligand, we planned synthesis of complexes with a less bulky $Tp^{R'}$ ligand, i.e., the Tp^{Me3} derivatives. Because the corresponding starting materials $Tp^{Me3}M-Cl$ (**1^{Me3}**) were not available, the nitrato and acetato complexes, $Tp^{Me3}Co(\kappa^2-NO_3)$ (**$1'^{Me3}$Co**) and $Tp^{Me3}Fe(\kappa^2-OAc)$ (**$1'^{Me3}$Fe**), were used instead.[19] Treatment of **$1'^{Me3}$Co,Fe** with appropriate Grignard reagents successfully produced the expected benzyl complexes **4^{Me3}Co,Fe**. Although the iron derivative **4^{Me3}Fe** could not be obtained in an analytically pure form due to its extreme sensitivity toward air, it was characterized by the chemical derivatization (carbonylation), as will be described below.

Finally we attempted and succeeded in the synthesis of $Tp^{R'}M-R$ complexes containing a normal alkyl group with β-hydrogen atoms: i.e., the ethyl complexes **6^{iPr2}Co,Fe** and **6^{Me3}Co**. The cobalt and iron complexes were blue and colorless, respectively, and the extremely

(19) See the introductory part of the following paper reported by us: Akita, M.; Ma, D.; Hikichi, S.; Moro-oka,Y. *J. Chem. Soc., Dalton Trans.* **1999**, 987.

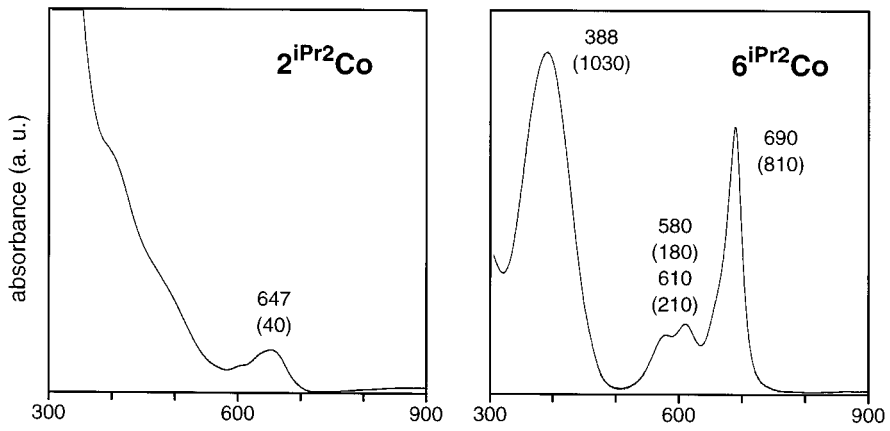

Figure 2. UV spectra of $Tp^{R'}Co$−hydrocarbyl complexes observed in toluene [λ_{max}/nm(ϵ/M^{-1} cm^{-1})]: (a, left) $Tp^{iPr2}Co$−η^3-allyl (**2^{iPr2}Co**). (b, right) $Tp^{iPr2}Co$−η^1-ethyl (**6^{iPr2}Co**).

Chart 2

M^{2+}	Fe (d^6)	Co (d^7)	Ni (d^8)
η^1	14e	15e	16e
η^3	16e	17e	18e

: observed

Scheme 2

$Tp^{iPr2}M$-Cl (**1^{iPr2}**) + R-MgX $\xrightarrow[\text{THF}]{\text{-78°C} \rightarrow \text{r.t.}}$ $Tp^{iPr2}M$-R (**4-6^{iPr2}**)

$Tp^{Me3}Co(\kappa^2\text{-}NO_3)$ (**$1'^{Me3}$Co**), $Tp^{Me3}Fe(\kappa^2\text{-}OAc)$ (**$1'^{Me3}$Fe**) + R-MgX $\xrightarrow[\text{THF}]{\text{-78°C} \rightarrow \text{r.t.}}$ $Tp^{Me3}M$-R (**4,6^{Me3}**)

	$Tp^{R'}$	M	R	Yield (%)
4^{iPr2}Fe	Tp^{iPr2}	Fe	*p*-methylbenzyl	68
4^{iPr2}Co	Tp^{iPr2}	Co		65
4^{iPr2}Ni	Tp^{iPr2}	Ni		0
4^{Me3}Fe	Tp^{Me3}	Fe		*
4^{Me3}Co	Tp^{Me3}	Co		65
5^{iPr2}Co	Tp^{iPr2}	Co	α-naphthylmethyl	75
6^{iPr2}Fe	Tp^{iPr2}	Fe	ethyl	79
6^{iPr2}Co	Tp^{iPr2}	Co		84
6^{iPr2}Ni	Tp^{iPr2}	Ni		0
6^{Me3}Co	Tp^{Me3}	Co		*

* Not isolated in a pure form. See text.

sensitive Tp^{Me3} derivatives were characterized by the chemical reactions (see below). To our surprise, the ethyl complexes **6Co,Fe** were very thermally stable despite the presence of β-hydrogen atoms, if they are kept under an inert atmosphere. Details of their chemical properties will be described below. While $Tp^{tBu,Me}Co$−R complexes were prepared by the reaction with organolithium reagents as reported by Theopold et al.,[6b] this method was unsuccessful for our system.

The obtained hydrocarbyl complexes **3**−**6Co,Fe** have been characterized by X-ray crystallography and various spectroscopic methods, the results of which are discussed in the following sections, and it has been verified

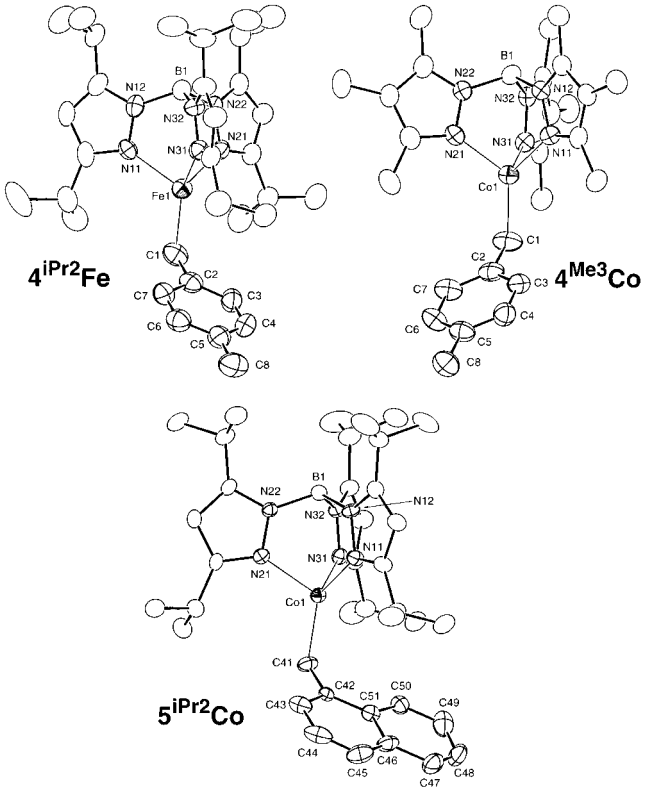

Figure 3. Molecular structures of $Tp^{R'}M$−benzyl-type complexes drawn at the 30% probability level.

that the obtained products are highly electron-deficient 14e (Fe) and 15e (Co) η^1-hydrocarbyl complexes.

X-ray Crystallography of η^1-Hydrocarbyl Complexes. Structural characterization has been performed for the *p*-methylbenzyl (**4^{iPr2}Fe** and **4^{Me3}Co**), α-naphthylmethyl (**5^{iPr2}Co**), and ethyl complexes (**6^{iPr2}Co**). ORTEP drawings are shown in Figures 3 and 4, and selected structural parameters of them are compared in Table 2 together with the two related methyl complexes $PhTp^{tBu}Fe$−Me (**VIII**)[6a] and $Tp^{tBu,Me}Co$−Me (**IX**)[6b] (Chart 3) and the chloro complex **1^{iPr2}Ni** (a reference of the tetrahedral species; one of the starting compounds). The result of preliminary X-ray crystallography of the iron complex **6^{iPr2}Fe**[20] is also shown in Figure 4.

First of all, all the hydrocarbyl complexes adopt virtually tetrahedral η^1 structures similar to the ally-

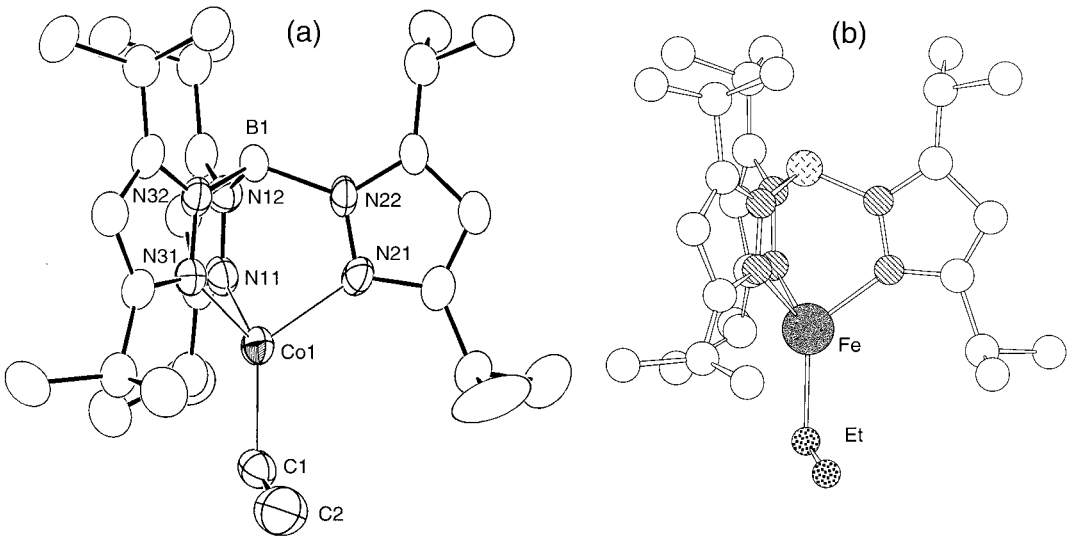

Figure 4. Molecular structures of Tp^{iPr2}M−ethyl complexes: (a) An ORTEP view of Tp^{iPr2}Co−Et (**6^{iPr2}Co**) drawn at the 30% probability level; (b) result of Fourier synthesis of Tp^{iPr2}Fe−Et (**6^{iPr2}Fe**).

Table 2. Selected Structural Parameters for Tp$^{R'}$M−R Complexes

	complex (R)						
	4^{iPr2}Fe (*p*-methylbenzyl)	**4^{Me3}Co** (*p*-methylbenzyl)	**5^{iPr2}Co** (α-naphthylmethyl)	**6^{iPr2}Co** (ethyl)	**VIII**[a] (methyl)	**IX**[b] (methyl)	**1^{iPr2}Ni** (Cl)
			Interatomic Distances (Å)				
M−C1(Cl)	2.06(1)	2.037(5)	2.042(6)	2.01(1)	2.079(3)	2.12(1)	2.172(2)
C1−C2	1.47(1)	1.476(9)	1.470(8)	1.36(3)			
M−C2	2.995(9)	3.074(8)	3.011(5)	2.89(3)	n.a.[d]	n.a.	
M−N11	2.055(7)	2.037(5)	2.019(4)	2.049(6)	2.138(2)	2.11(2)	1.975(3)
M−N21	2.057(7)	2.031(5)	2.037(4)	2.017(7)	2.103(2)	2.10(1)	1.978(4)
M−N31	2.088(6)	2.036(4)	2.045(5)	2.025(7)	2.132(3)	2.097(5)	1.965(4)
			Bond Angles (deg)				
N11−M−N21	87.5(3)	93.5(2)	91.3(2)	91.1(5)	88.18(8)	93.5(7)	92.5(1)
N11−M−N31	90.7(3)	91.8(2)	91.6(2)	92.7(5)	89.57(8)	93.8(6)	90.1(1)
N21−M−N31	90.3(2)	92.7(2)	93.5(2)	91.7(5)	90.61(8)	92.0(5)	92.0(2)
M−C1−C2	115.3(7)	123.2(4)	117.1(4)	117(2)			
N11−M−C1(Cl)	136.2(3)	130.1(3)	132.8(2)	123.1(3)	126.8(1)	122.6(6)	126.2(1)
N21−M−C1(Cl)	122.7(4)	125.6(3)	116.6(2)	125.2(3)	125.0(1)	122.2(7)	123.5(1)
N31−M−C1(Cl)	117.3(3)	113.0(2)	121.3(2)	124.5(3)	125.1(2)	124.3(6)	122.8(1)
B···M−C1(Cl) (θ_2)	11.0(4)	10.8(2)	10.3(2)	3.2(5)	n.a.	n.a.	0.9(1)
			Dihedral Angles (deg)				
N−M−C$_\alpha$−C$_\beta$ (θ_3)	9(1) [N11]	172.2(7) [N31]	6.6(7) [N11]	180(2) [N11]			
M−C$_\alpha$−C$_\beta$−C$_\gamma$ (θ_4)	−95(1)	−81(1)	89.5(6)				
	88(1)	99.4(8)	−91.7(6)				
Δ_4[c]	4	9	1.1				

[a] Reference 6a. [b] Reference 6b. [c] |(sum of the two θ_4 values)|/2. [d] n.a. = not available.

Chart 3

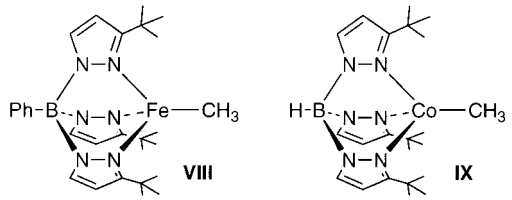

Chart 4

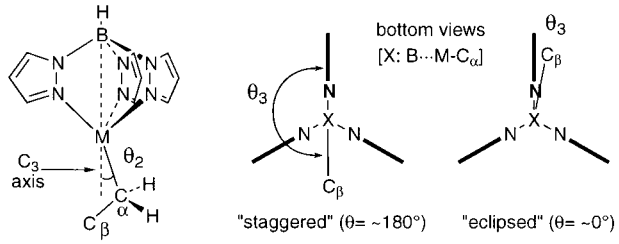

liron complex **2^{iPr2}Fe**. In addition, because parameters for the core parts of the two *p*-methylbenzyl complexes **4^{iPr2}Fe** and **4^{Me3}Co** are very similar, it is concluded that the bulky Tp^{iPr2} ligand does not cause significant structural deformation. In other words, kinetic stabilization (steric shielding) by a bulky ligand such as Tp^{iPr2} is not essential for the tetrahedral, coordinatively unsaturated Tp$^{R'}$M−R-type complexes.

As for the Tp$^{R'}$ moiety, the N−M−N angles (87−93°) close to the right angle and similar M−N distances (∼2.0 Å) indicate the virtually C_{3v}-symmetrical κ^3 coordination.

The M−C distances of ca. 2.0 Å fall in the typical ranges of metal−carbon single bonds of Fe and Co

(20) The structure could not be refined satisfactorily despite several attempts. The similarity of the structure was also supported by the cell parameters of **6^{iPr2}Fe** (a = 10.465(4) Å, b = 16.181(14) Å, c = 19.200(8) Å, β = 100.87(1)°, V = 3193(1) Å^3; cf. the parameters for **6^{iPr2}Co** in Table 5).

Chart 5

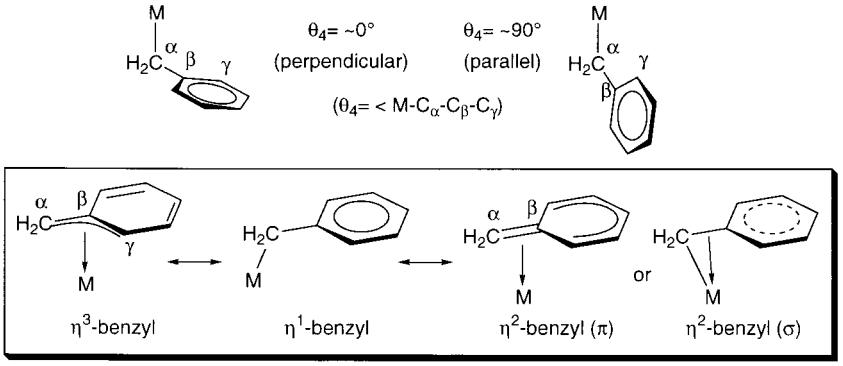

complexes.[4,5] When relative arrangements of the hydrocarbyl groups with respect to the $Tp^{R'}$ moieties are inspected in detail, the very small θ_2 value and the similar $C_\alpha-M-N$ angles (122−127°) of the ethyl (**6^{iPr2}Co**) and methyl derivatives (**VIII** and **IX**) (Table 2) reveal that their $[HB(C_3N_2)]_3M-C_\alpha$ parts are essentially C_{3v} symmetrical in a manner similar to the starting chloronickel complex **1^{iPr2}Ni**. In contrast to these complexes, the structures of the benzyl-type complexes **4** and **5^{iPr2}Co** are slightly deviated from C_{3v} symmetry judging from the corresponding parameters ($\theta_2 \approx 10°$; $\angle C_\alpha-M-N = 116-136°$). Because no significant interaction shorter than the sum of van der Waals radii of hydrogen atoms[21] is present between the hydrocarbyl and Tp^{iPr2} ligands, such structural deformation should not come from a steric interaction but from an electronic structure, as discussed below. The orientation of the CH_2-R group can be classified into two types readily differentiated by the torsion angle θ_3 (Chart 4): staggered conformation with $q_3 \approx 180°$ (**4^{Me3}Co** and **6^{iPr2}Co**) and eclipsed conformation with $\theta_3 \approx 0°$ (**4^{iPr2}Fe** and **5^{iPr2}Co**). Although nonbonded interactions of the α-hydrogen atoms of the hydrocarbyl groups with the $Tp^{R'}$ hydrogen atoms with distances of ca. 2.4 Å are found for all complexes, no systematic correlation with the conformation nor significant differences are detected for these two types of conformations. It is therefore concluded that (1) the two different conformations are caused by packing in single crystals and (2) because no intermediate θ_3 angle is found, the conformations may be a result of electronic structure (see below).

Let us discuss the orientation of the benzyl-type ligands in more detail. Here again, two conformations of the aromatic ring with respect to the $Tp^{R'}M$ part are possible as characterized by the dihedral angle $\angle M-C_\alpha-C_\beta-C_\gamma$ (θ_4; Chart 5 and Table 2). A deviation from the perpendicular conformation is best described by half of the sum of the two dihedral angles (Δ_4): the perpendicular conformation with $\Delta_4 \approx 0°$ vs the parallel form with $\Delta_4 \approx 90°$. The very small Δ_4 values for all the complexes (Table 2) clearly indicate the perpendicular conformations. In particular, because the Δ_4 value for **5^{iPr2}Co** containing the unsymmetrical naphthyl group is smallest, the conformation should be a result of electronic structures of the benzyl-type complexes. This is more support for the lack of severe steric repulsion between the aryl and $Tp^{R'}$ moieties.

(21) Emsley, J. *The Elements*, 3rd ed.; Oxford University Press: Oxford, U.K., 1998.

Chart 6

Three canonical structures are possible for benzyl complexes (η^1, η^2, and η^3; Chart 5), of which the η^3 structure can be eliminated on the basis of the virtually mirror-symmetrical structure of the $[HB(C_3N_2)_3]-M-CH_2C_6$ skeletons of the obtained complexes. The bending of the $B\cdots M-C_\alpha$ axis from an ideal C_{3v} structure (see above) and the parallel conformation of the aromatic rings should be a result of weak interaction between the benzyl moiety and the metal center. The electron-deficient metal center should be partially neutralized by donation of electrons from the benzyl group, and molecular orbital considerations (see below) reveal contribution of the σ-type structure rather than the π-type structure. Thus, the structural features of the benzyl-type complexes are best interpreted in terms of a resonance hybrid of the η^1 and η^2 forms, the former being dominant.

In contrast to the benzyl-type complexes, no significant structural deformation from a C_{3v} symmetry is observed for the alkyl complexes **6^{iPr2}Co**, **VIII**, and **IX**, as indicated by the $B\cdots M-C_\alpha$ angle close to 180° and the three similar $N-M-C_\alpha$ angles. If agostic interactions[2] of the alkyl ligand with the electron-deficient metal center occur as shown in Chart 6, (1) the $M-C_\alpha-C_\beta$ angle should become obtuse (θ_α in α-agostic interaction) or acute (θ_β in β-agostic interaction) and (2) the $M-C_\alpha$ vector should become unsymmetrical with respect to the $Tp^{R'}M$ backbone. Actually, because (1) the $M-C_\alpha-C_\beta$ angle of the ethyl complex **6^{iPr2}Co** (117°) is close to the bond angle ideal for a sp^3-hybridized carbon atom (109°) and (2) the $M-C_\alpha$ vector of the three alkyl complexes is virtually superimposed on the C_{3v} axis of the $[HB(C_3N_2)_3]M$ moiety, such agostic interactions are absent for these complexes. These considerations lead to the conclusions that (1) the alkyl ligands in **6^{iPr2}Co**, **VIII**, and **IX** are interacted with the metal centers only through the $M-C$ σ-bond and (2) additional interactions such as steric shielding by the $Tp^{R'}$ ligand and agostic interactions do not contribute to stabilization of the highly electron-deficient 14e (Fe) and 15e (Co) species.

Spectroscopic Characterization of η^1-Hydrocarbyl Complexes. The hydrocarbyl complexes obtained

Table 3. Selected Spectroscopic Data for Hydrocarbyl Complexes, $Tp^{R'}M$-R

complex	ν(BH)[a]	UV−vis λ_{max}/nm (ϵ)[b]	μ_{eff}/μ_B[c]	spin state
2^{iPr2}Co (η^3)	2536	647 (40)	1.8	d^7 low spin
4^{iPr2}Co (η^1)	2545	347 (1430), 457 (1150), 591 (360), 630 (370), 696 (1130)	4.2	d^7 high spin
4^{Me3}Co (η^1)	2519	342 (1690), 450 (1520), 592 (390), 628 (450), 695 (1140)	4.2	d^7 high spin
5^{iPr2}Co (η^1)	2545	422 (2860), 504 (900), 541 (660), 601 (610), 640 (630), 703 (1700)	4.1	d^7 high spin
6^{iPr2}Co (η^1)	2543	388 (1030) 580 (180), 610 (210), 690 (810)	4.2	d^7 high spin
2^{iPr2}Fe (η^1)	2543	*d*	5.0	d^6 high spin
4^{iPr2}Fe (η^1)	2544	*d*	4.9	d^6 high spin
6^{iPr2}Fe (η^1)	2541	*d*	5.0	d^6 high spin

[a] KBr pellets. [b] Observed in toluene for Tp^{iPr2} complexes and in hexane for **4^{Me3}Co**. [c] Solid samples at room temperature. [d] No characteristic absorption.

by the present study were also characterized by spectroscopic methods, and selected spectroscopic data for the cobalt and iron complexes are summarized in Table 3. Except the η^3-allylcobalt complex **2^{iPr2}Co**, all other complexes are η^1-hydrocarbyl complexes, spectroscopic data of which are consistent with the results of the structural characterization mentioned above.

(i) Cobalt Complexes. The (η^1-hydrocarbyl)cobalt complexes are characterized on the basis of the results of IR, UV, magnetic susceptibility, and ^{1}H NMR measurements.

The ν_{BH} vibrations appear in the range of 2519−2545 cm^{-1}, typical for κ^3 coordination of the $Tp^{R'}$ ligand.[10d]

The green-blue color of **4**−**6Co** is definitely different from the dark orange color of the η^3-allyl complex **2^{iPr2}Co**, suggesting a geometry dissimilar to that of **2^{iPr2}Co**. Our previous study revealed that tetrahedral $Tp^{R'}$Co−X species show characteristic UV features, i.e., a few d−d transitions observed around 500−600 nm (the origin of the blue-green color). For example, the tetrahedral cumylperoxo complex $Tp^{tBu,iPr}$Co−η^1-$OOCMe_2Ph$,[10a] which was characterized as a tetrahedral species by X-ray crystallography, shows the following UV−vis absorptions: λ_{max}/nm (ϵ/M^{-1} cm^{-1}) 350 (sh, 250), 549 (370), 597 (590), 663 (1160). The UV−vis spectrum of **6^{iPr2}Co** given as a typical example of hydrocarbylcobalt complexes (Figure 2b) is completely different from that of the allyl complex **2^{iPr2}Co** (Figure 2a) but very similar to that of $Tp^{tBu,iPr}$Co−η^1-$OOCMe_2Ph$, suggesting a similar tetrahedral structure. In contrast to the square-pyramidal **2^{iPr2}Co** complex with a low-spin configuration, tetrahedral species should have a high-spin configuration of d electrons, which is confirmed by measurement of magnetic susceptibility. The effective magnetic moments (μ_{eff}) of the hydrocarbyl complexes **4**−**6Co** (4.1−4.2) are much larger than for the allyl complex **2^{iPr2}Co** (1.8 μ_B), and the values are consistent with quartet states ($S = {}^3/_2$) containing three unpaired d electrons. Although the μ_{eff} values are larger than the spin-only moment for $S = {}^3/_2$ (3.9 μ_B), it is well-known that contribution of an orbital angular momentum causes such an increase.[18] The high-spin species give isotropically shifted ^{1}H NMR spectra. Lack of coupling information prevents assignments of weak signals, and signals for hydrogen atoms close to the metal center are not usually observed but the small number of the intense methyl signals (2 (18H each) for Tp^{iPr2}; 3 (9H each) for Tp^{Me3}) supports the C_{3v}-symmetrical structure.

These spectroscopic data are consistent with the tetrahedral (κ^3-$Tp^{R'}$)Co−η^1-R structure with a high-spin configuration of d electrons, and a combination of these spectroscopic methods is a useful diagnosis for such species.

(ii) Iron Complexes. The (η^1-hydrocarbyl)iron complexes are also characterized spectroscopically, although they are more featureless than the cobalt analogues. The pale yellow iron complexes **4,6^{iPr2}Fe** show no characteristic UV−vis feature, and their tetrahedral structures were supported by the data of IR ($\nu_{BH} \rightarrow \kappa^3$), magnetic susceptibility ($\mu_{eff} = \sim 5.0 \rightarrow$ quintet high spin ($S = 2$)) and ^{1}H NMR measurements (a single set of two methyl signals (each 18H) $\rightarrow C_{3v}$ symmetry).

Reactivity of $Tp^{R'}M$−R-type Hydrocarbyl Complexes. Three types of reactivity of the coordinatively unsaturated hydrocarbyl complexes **2**, **4**- and **6Fe,Co** were studied. A series of reactions to determine their thermal stability and to confirm the presence of a metal−carbon bond in them was carried out at first and then the reactivity of the novel complexes toward organic compounds was studied.

(i) Thermolysis of Ethyl Complexes 6Fe,Co. It is remarkable that the ethyl complexes **6Fe,Co** were resistant to β-hydride elimination. When a heptane solution of **6Fe,Co** was heated for 5 h at 110 °C, only a trace amount of ethene, the product of β-hydride elimination, was detected by GLC analysis of the gas phase (eq 3). Formation of ethane should be due to hydrolysis

$$\underset{\mathbf{6}}{Tp^{R'}M\text{-}CH_2CH_3} \xrightarrow[\text{heptane}]{110\,^\circ C,\ 5\ h} CH_3\text{-}CH_3 + CH_2{=}CH_2 \qquad (3)$$

	CH_3-CH_3	CH_2=CH_2
6^{iPr2}Fe	10	< 1
6^{iPr2}Co	8	< 1
6^{Me3}Co	20	6

Yields (%) were determined by GLC.

with adventitious moisture in the reaction system, because the yield was constant from the initial stage of thermolysis and virtually independent of the heating time.

Although ethane formation was not detected by GLC analysis, ^{1}H NMR monitoring revealed occurrence of some decomposition of the cobalt complex **6^{iPr2}Co**. At 60 °C no apparent change was observed but heating at 120 °C caused complete decomposition after 11 h to give a single unidentified species. Thus, **6^{iPr2}Co** follows a decomposition pathway, which does not afford ethene as a byproduct. The iron complex **6^{iPr2}Fe** was robust, because no spectral change was observed even after heating for 4 h at 110 °C.

Despite the highly electron deficient nature, the ethyl complexes **6Fe,Co** are resistant to β-hydride elimination, a typical thermal decomposition pathway for coordinatively unsaturated hydrocarbyl complexes bearing β-hydrogen atoms, and the thermal stability is found to be an intrinsic property of $Tp^{R'}M$−R-type compounds.

Theopold reported the more thermally stable derivative $Tp^{tBu,Me}Co-n$-Bu (stable for weeks at 90 °C; a derivative of **IX**),[6b] and the stability was ascribed to steric protection by the bulky $Tp^{tBu,Me}$ ligand.

(ii) Protonation and Hydrogenolysis. Treatment of **4** and **6** with protic acids such as HCl(aq) and acetic acid afforded the corresponding alkanes in good yields, as shown in eq 4. When acetic acid was used,

$$Tp^{R'}M\text{-}R \xrightarrow[\text{toluene}]{H^+ \text{ or } H_2} R\text{-}H \qquad (4)$$

2, **4**, **6**

complex	R / product (R-H)	protonolysis	hydrogenolysis
2^{iPr2}**Fe**	allyl / propene	66 [b]	44
2^{iPr2}**Co**		79 [b]	35
2^{iPr2}**Ni**		0 [b]	0
4^{iPr2}**Fe**	*p*-methylbenzyl / *p*-xylene	91 [c]	78
4^{iPr2}**Co**		94 [c]	82
4^{Me3}**Co**		81 [c]	67
6^{iPr2}**Fe**	ethyl / ethane	90 [c]	87
6^{iPr2}**Co**		92 [c]	91
6^{Me3}**Co**		85 [c]	80

[a] Protonolysis was performed in toluene for 30 min at r.t. Hydrogenolysis was performed in toluene at r.t. under H_2 atmosphere (2^{iPr2}: H_2 1 atm, for 12 hrs; **4**, **6**: H_2 2 atm, for 1 hr). Yields were determined by GLC. [b] with acetic acid. [c] with aqueous HCl.

$Tp^{R'}M(\kappa^2\text{-OAc})$ species were isolated from the residues. The alkanes were also produced upon hydrogenolysis (2 atm). Although the organometallic products of the hydrogenolysis are anticipated to be hydrides, $Tp^{R'}M-H$, the residue did not show any absorption assignable to a ν_{M-H} vibration in the range of 2100−1500 cm^{-1} [2] (cf. $Tp^{tBu,Me}Co-H$: 1669 cm^{-1})[6b] and the dark brown color of the mixture obtained from the cobalt complex was different from the blue color of $Tp^{tBu,Me}Co-H$. Attempted synthesis of $Tp^{iPr2}Co-H$ by treatment of $\mathbf{1^{Pr2}Co}$ with hydride reagents ($NaBH_4$, $LiAlH_4$, $LiHBEt_3$) was unsuccessful.

(iii) Carbonylation. The iron complexes **2**-, **4**-, and **6Fe** were readily carbonylated under CO atmosphere (1 atm) to give yellow products **7** (eq 5), which were readily characterized as acyl-dicarbonyl complexes on the basis of the $\nu_{C=O}$ and two ν_{CO} vibrations observed around 1600 and 2000 cm^{-1}, respectively. The diamag-

$$Tp^{R'}Fe\text{-}R \xrightarrow{CO\ (1\ atm)} \mathbf{7} \qquad (5)$$

R'	R	products
i-Pr_2	allyl	**7a** [from 2^{iPr2}**Fe**]*
	p-methylbenzyl	**7b** [54 % yield; from 4^{iPr2}**Fe**]
	ethyl	**7c** [62 % yield; from 6^{iPr2}**Fe**]
Me_3	*p*-methylbenzyl	**7d** [63 % yield; from 4^{Me3}**Fe**]

*: A pure sample could not be obtained.

netic products **7** are also characterized by the NMR data, and acyl C=O signals around δ_C 250 are observed in addition to CO signals. The 1:2 pattern of the $pz^{R'}$ signals suggests a mirror-symmetrical structure. These data are consistent with the octahedral structure coordinated by κ^3-$Tp^{R'}$ (ν_{BH} >2500 cm^{-1}), η^1-acyl, and two CO ligands. The two sets of $\nu_{C=O}$ and ν_{CO} vibrations observed for the two complexes $Tp^{iPr2}Fe(CO)_2C(=O)Et$ (**7b**) and $Tp^{Me3}Fe(CO)_2C(=O)$-$CH_2C_6H_5Me$-*p* (**7c**) indicated the presence of two components. Furthermore, the NMR signals for the $CH_2C(=O)Fe(CO)_2$ moiety of **7d**, which could not be located at room temperature, appeared as two sets of signals in a 1.0:0.8 ratio upon cooling at −70 °C. These changes suggest occurrence of a dynamic behavior similar to that for the acetyl complex $Tp^{H}Fe(CO)_2C(=O)Me$, reported by Cotton more than 20 years ago.[22] In the present case, too, the temperature-dependent, hindered rotation of the Fe−acyl bond should result from the Fe−C double-bond character due to contribution of the oxycarbene resonance form $[Fe^+=C(O^-)R]$.[2]

The acyl complex should be formed by way of the alkyl complex $Tp^{R'}Fe(CO)_2-R$. When the carbonylation of $\mathbf{6^{iPr2}Fe}$ was monitored by ^1H NMR, an intermediate showing 1:2 4-pz-H signals (δ_H 6.06 (2H), 5.92 (1H)) was detected and was gradually converted to **7c**. This diamagnetic species might be assigned to the alkyl intermediate, $Tp^{iPr2}Fe(CO)_2Et$, but the ethyl ligand signals could not be located, probably due to overlapping with the bristling methyl signals of the pz^{iPr2} rings.

Carbonylation of the cobalt complexes also afforded dark brown acyl-monocarbonyl complexes **8**, which were each characterized by one $\nu_{C=O}$ and one ν_{CO} absorption (eq 6). Although the propanoyl complexes **8c**,**e** were

$$Tp^{R'}Co\text{-}R \xrightarrow[\text{hexane}]{CO\ (1\ atm)} \mathbf{8} \qquad (6)$$

2,**4**,**6**$^{R'}$**Co**

R'	R		ν(B-H) [b]	ν(CO) [b]	ν(C=O) [b]
iPr_2	allyl	**8a** [from 2^{iPr2}**Co**] [a]	2538	2005	1647
	p-methylbenzyl	**8b** [from 4^{iPr2}**Co**] [a]	2536	2006	1654
	ethyl	**8c** [from 6^{iPr2}**Co**]	2540	1999	1636
Me_3	*p*-methylbenzyl	**8d** [from 4^{Me3}**Co**] [a]	2523	2006	1653
	ethyl	**8e** [from 6^{Me3}**Co**]	2524	1994	1642

[a] Further decomposition was observed. See text. [b] in cm^{-1}; **8c**,**e**: KBr pellets; **8a**,**b**,**d**: hexane solutions.

stable, the other products decomposed upon removal of the volatiles under reduced pressure to result in the green product **9**, which did not show an acyl C=O vibration but a single CO absorption around 1950 cm^{-1} irrespective of the R group in the starting complexes. Product **9**, which could not be isolated in a pure form, was assigned as $Tp^{R'}Co^{I}-CO$ by comparison with related complexes (R′ = iPr, Me; neopentyl)[23] and the Co(I) species should be formed by way of homolysis of a Co−organyl bond. Of two possible candidates, i.e., the carbonylated product $[Tp^{R'}Co(CO)R]$ or the acylated product $[Tp^{R'}Co(CO)C(=O)R]$, the former may be the intermediate of the Co−C homolysis, because (1) the homolysis process depends on R and (2) complexes bearing an R group, which can stabilize the correspond-

(22) Cotton, F. A.; Frenz, B. A.; Shaver, A. *Inorg. Chim. Acta* **1973**, *7*, 161.
(23) Detrich, J. L.; Konecny, R.; Vetter, W. M.; Doren, D.; Rheingold, A. L.; Theopold, K. H. *J. Am. Chem. Soc.* **1996**, *118*, 1703.

ing radical species R•, undergo the homolysis easily (Et vs allyl and benzyl). The methyl complexes **VIII** and **IX** were reported to be converted to the corresponding $Tp^{R'}M^{I}-CO$ species upon carbonylation,[6] and the facile $M-CH_3$ homolysis processes were ascribed to the bulky $Tp^{R'}$ ligands bearing *t*-Bu groups at the 3-positions proximal to the metal center.

Thus, hitherto discussed protonation, hydrogenolysis, and carbonylation serve as useful methods to detect hydrocarbyl species.

(iv) Trapping of η^1-Hydrocarbylnickel Intermediate by CO. In contrast to the Co and Fe systems, the corresponding Ni species, $Tp^{iPr2}Ni-R$, could not be obtained as mentioned above. We then attempted trapping of the putative alkyl intermediate by CO.

When EtMgBr was added to a THF solution of **1^{iPr2}Ni** at −78 °C, the reaction mixture changed from pink to green (eq 7). Neither ethene nor ethane was detected

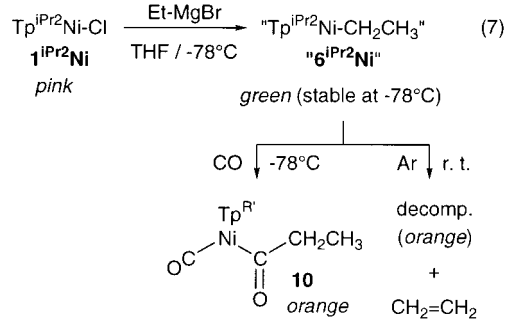

(7)

in the gas phase. During warming to room temperature the mixture turned orange, and at room temperature quantitative formation of ethene was confirmed by GLC analysis. This result was in sharp contrast to the results of the Fe and Co systems, which produced ethene in less than 20% yield. These results suggested that, in the case of the Ni system, the ethyl intermediate underwent β-hydride elimination at room temperature to give ethene.

To trap the intermediate, the reaction mixture was carbonylated at −78 °C before warming to room temperature and orange diamagnetic product **10** was isolated in 71% yield. Complex **10** was also obtained by alkylation of **1^{iPr2}Ni** under a CO atmosphere (1 atm) at −78 °C. Its IR features ($\nu_{C=O}$ 1682, ν_{CO} 2009, ν_{BH} 2547 cm^{-1}) are very similar to those of the Co analogue **8c**, and NMR data ((1) a single set of averaged **pz^{iPr2}** signals, (2) δ_C(C═O) 226 and δ_C(C≡O) 187) also confirmed formation of the analogous acyl−monocarbonyl species **10**, $Tp^{iPr2}Ni(CO)C(=O)Et$, which was confirmed by X-ray crystallography. An ORTEP view is shown in Figure 5 and selected structural parameters are listed in Table 4. The acyl complex **10** adopts a trigonal-bypiramidal structure. The facial Tp^{iPr2} ligand occupies two of the three equatorial sites and one of the two axial sites, and the acyl and carbonyl ligands are coordinated to the remaining axial and equatorial positions, respectively. In accord with this geometry, the equatorial N21−Ni1−N31 angle is much smaller than the other two N−Ni−N angles spanning the axial and equatorial sites, and the more π-accepting acyl ligand occupies the axial position, where back-donation occurs more effectively than at the equatorial site.[24] The averaged ^{1}H NMR signals for the pz^{iPr2} rings indicates pseudorotation of the Tp^{iPr2} ring.[13]

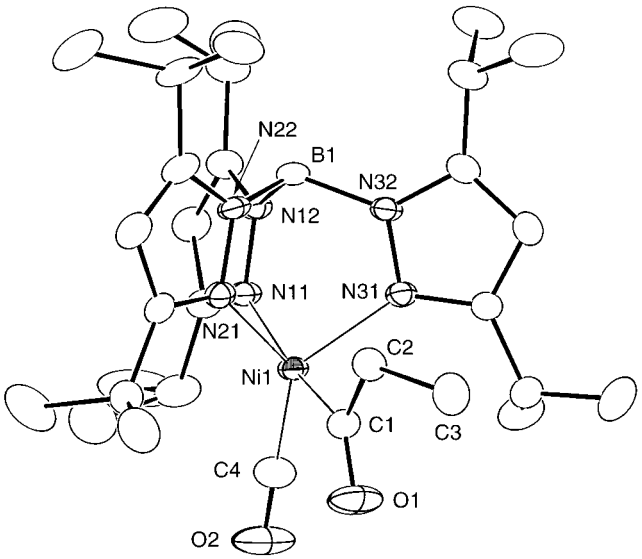

Figure 5. Molecular structure of **10** drawn at the 30% probability level.

Table 4. Selected Structural Parameters for 10

Bond Lengths (Å)			
Ni1−N11	2.057(3)	O1−C1	1.195(5)
Ni1−N21	2.009(3)	O2−C4	1.123(6)
Ni1−N31	2.032(3)	C1−C2	1.526(6)
Ni1−C1	1.947(4)	C2−C3	1.516(6)
Ni1−C4	1.764(5)		
Bond Angles (deg)			
N11−Ni1−N21	85.3(1)	N31−Ni1−C4	129.6(2)
N11−Ni1−N31	86.7(1)	C1−Ni1−C4	87.3(2)
N21−Ni1−N31	98.9(1)	Ni1−C1−O1	124.0(3)
N11−Ni1−C1	171.7(2)	Ni1−C1−C2	115.9(3)
N11−Ni1−C4	101.0(2)	O1−C1−C2	120.1(4)
N21−Ni1−C1	89.6(2)	C1−C2−C3	112.5(4)
N21−Ni1−C4	131.2(2)	Ni1−C4−O2	176.7(5)
N31−Ni1−C1	87.7(1)		

Thus, the putative ethylnickel species **6^{iPr2}Ni** was successfully trapped by CO and the above-mentioned reaction pathway could be confirmed experimentally. Although formation of analogous acyl species was indicated for the *p*-methylbenzyl species $Tp^{iPr2}Ni-CH_2C_6H_4$-*p*-Me (**4^{iPr2}Ni**) by IR monitoring of the reaction mixture (ν_{CO} 2015 cm^{-1}; $\nu_{C=O}$ 1696 cm^{-1}), it decomposed upon removal of the volatiles.

(v) Oxygenation. Exposure of a toluene solution of **2, 4**, or **6** to O_2 resulted in instantaneous oxygenation, as shown in eq 8. The reaction of the complexes without β-hydrogen atoms, **2** and **4**, afforded the corresponding aldehydes [R″-CHO(R″CH_2 = R)] exclusively, whereas the ethyl complexes **6** produced a mixture of ethanol, acetaldehyde, and acetic acid. Dinuclear μ-hydroxo complexes, $(Tp^{R'}M)_2(\mu\text{-}OH)_2$, were formed as the only inorganic products, as indicated by ^{1}H NMR monitoring of the reaction.

The oxygenation was followed by UV spectroscopy using the (η^3-allyl)cobalt complex **2^{iPr2}Co**, because a tetrahedral η^1 intermediate, which should show UV features distinct from those of the square-pyramidal **2^{iPr2}Co**, was anticipated to be detected. Exposure of a toluene solution of **2^{iPr2}Co** to O_2 at −78 °C caused a

(24) See refs 2 and 17.

$$Tp^{R'}M\text{-}R \xrightarrow[\text{toluene}]{O_2} R''\text{-}CHO \text{ etc.} \quad (R = CH_2R'') \qquad (8)$$

complex	R	product(s)	yield (%)
$\mathbf{2^{iPr2}Fe}$	allyl	CH_2=CHCHO	52
$\mathbf{2^{iPr2}Co}$	allyl	CH_2=CHCHO	87
$\mathbf{2^{iPr2}Ni}$	allyl	CH_2=CHCHO	80
$\mathbf{4^{iPr2}Fe}$	*p*-methylbenzyl	*p*-tolualdehyde	82
$\mathbf{4^{iPr2}Co}$	*p*-methylbenzyl	*p*-tolualdehyde	84
$\mathbf{4^{Me3}Co}$	*p*-methylbenzyl	*p*-tolualdehyde	75
$\mathbf{6^{iPr2}Fe}$	ethyl	CH_3CH_2OH	24,[b] 8,[c] 10 [d]
$\mathbf{6^{iPr2}Co}$	ethyl	CH_3CHO	17,[b] 29,[c] 12 [d]
$\mathbf{6^{Me3}Co}$	ethyl	CH_3COOH	5,[b] 10,[c] 5 [d]

[a] Toluene solutions were stirred under O_2 atmosphere (-78°C → r.t.). Yields were determined by GLC. [b] yield of ethanol. [c] yield of acetaldehyde. [d] yield of acetic acid.

color change to pale blue and appearance of UV absorptions (λ_{max} = 634, 575 nm) indicative of formation of a tetrahedral species (cf. $Tp^{iPr2}Co$−OO-cumyl: λ_{max} = 638, 582 nm).[10a] When the mixture was warmed to ambient temperature, the absorptions disappeared. The transient pale blue species could be the tetrahedral allylperoxo species $Tp^{iPr2}Co$−OO-allyl, resulting from O_2 insertion into the Co−C bond.

Thus, the M−C bonds in $Tp^{R'}M$−R are susceptible to O_2 insertion to give alkylperoxo species, $Tp^{R'}M$−OOR. O−O homolysis and H-abstraction from R−O• by Tp^{iPr2}-Co−O• should give aldehyde, as discussed in ref 10a.

(vi) Reaction with Unsaturated Organic Compounds. Reactivity of coordinatively unsaturated hydrocarbyl complexes has attracted much attention, because they are key intermediates of catalytic C−C bond formation. In particular, the recent, independent reports by Brookhart and Gibson[25] on the polymerization catalysts containing PBI (pyridinebis(imine)) ligands with bulky substituents recalled our interests to development of novel catalyst systems based on N-coordinated precursors. Both of the PBI and $Tp^{R'}$ ligands are κ^3-N-coordinated ligands, but their coordination geometry is different: i.e., meridional (PBI) vs facial ($Tp^{R'}$). In addition, the former ligands are neutral, whereas the latter ligands are mononegative species. It is therefore interesting to compare their catalytic activity toward olefin polymerization. The experiments described below, however, reveal that the $Tp^{R'}M$ complexes are sluggish with respect to reactions with unsaturated organic compounds including olefin and acetylene.

Reactivity of the ethyl complexes $\mathbf{6^{iPr2}}$ is described in detail as typical examples of the hydrocarbyl complexes. Toluene solutions containing $\mathbf{6^{iPr2}}$ were heated for 1 h at 70 °C in the presence of various organic compounds, and the resultant mixtures were subjected to GLC analysis after hydrolysis with aqueous HCl solution. Of the examined organic compounds (ethene, 1-butene, ethyl acrylate, styrene; phenylacetylene, diphenylacetylene; diethyl ketone; benzonitrile) only phenylacetylene showed indication of some reaction and the other

Scheme 3

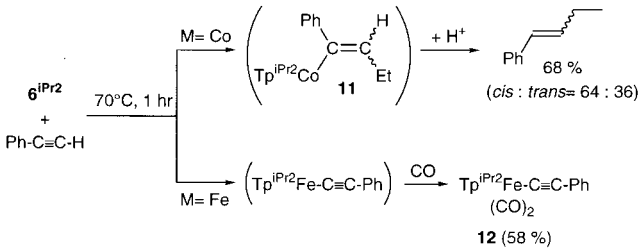

substrates left $\mathbf{6^{iPr2}}$ unaffected (Scheme 3). Reaction of $\mathbf{6^{iPr2}Co}$ with phenylacetylene gave an isomeric mixture of *cis*- and *trans*-1-phenyl-1-butene in 68% yield after hydrolysis. The olefinic product should arise from insertion of the C≡C bond into the Co−Et bond followed by protonolysis of the Co−C(sp^2) bond in the resultant alkenyl complex **11**. Reaction of the iron derivative $\mathbf{6^{iPr2}Fe}$ contrasted with the result of $\mathbf{6^{iPr2}Co}$. Treatment with phenylacetylene followed by carbonylation gave the diamagnetic product **12**, which was analyzed as an acetylide−dicarbonyl complex on the basis of the spectroscopic data (see Experimental Section). Thus, the reaction of $\mathbf{6^{iPr2}Fe}$ with PhC≡CH should result in protonolysis of the Fe−Et bond with the acidic acetylenic proton followed by coordination of the resulting conjugated base (acetylide ligand) to the metal center to give the acetylide complex, Tp^{iPr2}Fe−C≡CPh, carbonylation of which should lead to **12**.

Preliminary experiments on catalytic ethene polymerization were also carried out using the chloro ($\mathbf{1^{iPr2}Fe}$,$\mathbf{Co}$) and ethyl complexes ($\mathbf{6^{iPr2}Fe}$,$\mathbf{Co}$). Although no catalytic activity was observed as they were, addition of MAO (100 equiv) caused production of polyethylene. The activities, however, were much smaller ($<10^{-4}$) than those reported for the PBI catalyst.[25] Although interaction between $\mathbf{6^{iPr2}Co}$ and ethene was monitored by ^{1}H NMR (at room temperature and 50 °C), no positive result was obtained.

Despite the highly coordinatively unsaturated electronic structures of the $Tp^{R'}M$−R-type hydrocarbyl complexes, their reactivity turns out to be sluggish with respect to C−C bond formation with unsaturated organic compounds. The contrasted catalytic activity for ethene polymerization by the PBI and $Tp^{R'}$ systems suggests that facially coordinated N_3 ligands may not be suitable as catalytic species.

EHMO Analysis of $Tp^{R'}M$−R. To examine the reason for the stability of the hydrocarbyl complexes, EHMO calculations were performed for the idealized C_{3v}-symmetrical model methyl complexes $Tp^{H}M$−Me (**A**; M = Fe, Co). A molecular orbital diagram of **A-Fe** resulting from interaction between Tp^{H}Fe and Me fragments is shown in Figure 6. Because a very similar diagram is obtained for the cobalt complex **A-Co**, electronic structures of the two complexes will be discussed together. The diagram is essentially the same as those reported for the TpCo(I) species by Theopold et al.[23]

At first glance the diagram is very simple, because the $Tp^{H}M$ fragments have only one σ-type orbital that can interact with the methyl σ-orbital. This situation is in sharp contrast to that of normal organometallic species such as Me−$Co(CO)_4$, where two metal d-based

(25) (a) Ittel, S. D.; Johnson, L. K.; Brookhart, M. *Chem. Rev.* **2000**, *100*, 1169. (b) Britovsek, G. J. P.; Gibson, V.; Wass, D. F. *Angew. Chem., Int. Ed.* **1999**, *38*, 428.

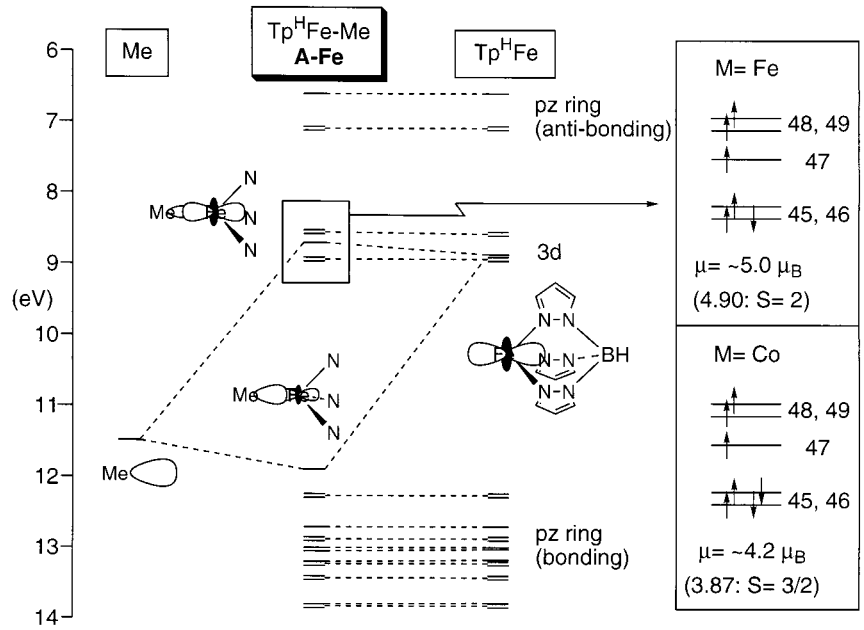

Figure 6. MO diagram for Tp^HM-Et (**A**) resulting from the interaction between Me and Tp^HM fragments.

orbitals take part in the M−C interaction to form a strong σ bond (for comparison, see Figure S1). As a result, the very small mixing of the orbitals of σ-symmetry in the Tp^HM systems renders the bond less covalent. In other words, the M−C bond in **A** is ionic, and this result is in accord with the high sensitivity of $Tp^{R'}M-R$ toward moisture.

The very small energy separation between frontier orbitals would lead to a high-spin configuration as usually observed for tetrahedral metal species.[18] When 6 (Fe) and 7 electrons (Co) are accommodated in the 5 frontier orbitals, 4 (Fe) and 3 unpaired electrons (Co) will remain in the orbitals 46−49 of higher energies. These pictures of electron configurations are in good agreement with the results of measurements of magnetic moment. The observed values of effective magnetic moment (μ_{eff} = ~5.0 μ_B (Fe), ~4.2 μ_B (Co); see above) are typical for $S = 2$ (Fe) and $^3/_2$ (Co), respectively, as described above.

The electronic configuration displayed in Figure 6 can also explain the stability of the tetrahedral, coordinatively unsaturated species. When the "18e rule"[2] is taken into account, the 14e (**A-Fe**) and 15e species (**A-Co**) are short of valence electrons by 4 and 3 electrons, respectively. However, all frontier orbitals are occupied either by electron pairs or by unpaired electrons, meaning that no vacant frontier (d) orbital for coordination of an additional ligand is left any more. The lack of vacant coordination site is concluded to be the origin of the stability of the highly coordinatively unsaturated organometallic species. It may be impossible for unsaturated hydrocarbons to be coordinated to the metal centers without changing the electronic structure. The electronic structures, however, are not so rigid, because CO, H_2, and O_2 react with these species. Substrates, which can perturb the electronic structure of the $Tp^{R'}M-R$ complexes, may have a chance to show some new reactivity.

Let us add a note on the carbonylation, which occasionally results in reduction of the metal center to give the M^I-CO species via M−C homolysis as discussed above. If CO is coordinated to the metal center (i.e., two electrons are added to **A**), orbital 47 will be occupied by an electron pair. Because orbital 47 bears the M−C antibonding character, two-electron addition would cause cleavage of the M−C bond.

Chart 7

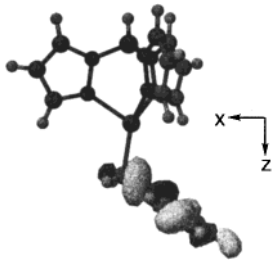

It has been known that carbon ligands cause ligand-field splitting much larger than N-, O-, and halo-ligands, which are typical ligands for coordination compounds.[18] The present study reveals that the σ-bonding interaction of carbon ligands is not enough to cause a low-spin configuration with vacant frontier orbitals by lifting up the M−C antibonding orbital. Some additional interaction with an orbital of higher energy is essential to form a low spin-species with a vacant coordination site as observed for $Me-Co(CO)_4$.

The distortion of the benzyl-type complexes **4** and **5** can also be rationalized by the interaction of the filled σ-type orbital with the d_{xz}-type metal d orbital, as shown for Tp^HFe-CH_2Ph in Chart 7.[26a] The CH_2-Ph σ-orbital is drifting toward the metal center to neutralize the electron deficient metal center.[26b]

We also carried out a comparison of $Tp^HM-\eta^1$-allyl and $Tp^HM-\eta^3$-allyl (M = Fe, Co, Ni). However, in every case the η^3 structures are found to be more stable than the η^1 structure, due to effective back-donation to the nonbonding π-orbital of the η^3-allyl ligand, and thus the

(26) (a) The d_{xz} orbital cannot be seen due to its small contribution. (b) Essentially the same result was obtained from preliminary DFT calculations on $\mathbf{4^{Me3}Co}$.

experimental results have not been reproduced at the level of EHMO calculation.

Conclusions. The tetrahedral (η^1-hydrocarbyl)iron and -cobalt complexes $Tp^{R'}M-R$ (**2**, **4**−**6**), bearing the $Tp^{R'}$ auxiliary as the only ancillary ligand, are successfully prepared and characterized by means of spectroscopic and crystallographic methods. Despite their highly unsaturated electronic structures (14e (Fe), 15e (Co)), they are thermally stable under an inert atmosphere, and it is remarkable that the ethyl complexes **6** containing β-hydrogen atoms do not undergo β-hydride elimination, which has been regarded as a common decomposition pathway of normal coordinatively unsaturated hydrocarbyl complexes. The presence of a M−C bond is confirmed by chemical reactions such as protonolysis, hydrogenolysis, oxygenation, and carbonylation. The reactivity of $Tp^{R'}M-R$ toward unsaturated organic substrates, including olefin and acetylene, turns out to be sluggish and insertion is observed only for PhC≡CH (with $Tp^{iPr2}Co-Et$). On the basis of the results of EHMO calculations the stability of $Tp^{R'}M-R$ is attributed to the high-spin electronic configuration, where all the frontier orbitals are occupied by an electron pair or an unpaired electron.

Experimental Section

General Methods. All manipulations were carried out under an Ar atmosphere using standard Schlenk tube techniques. THF, ether, toluene, pentane, and hexane were dried over Na−K/benzophenone under Ar and distilled just before use. NMR spectra were recorded on Bruker AC200 (^{1}H, 200 MHz), JEOL EX-270 (^{1}H, 270 MHz, variable-temperature measurements) and JEOL EX-400 spectrometers (^{1}H, 400 MHz, variable-temperature measurements; ^{13}C, 100 MHz). Benzene-d_6 and toluene-d_8 for NMR measurements containing 0.5% TMS were dried over Na−K and distilled under reduced pressure. IR and UV spectra were obtained on JASCO FT/IR 5300 and V-570 spectrometers, respectively. The oxygenation of **2^{iPr2}Co** at low temperature was monitored using a multichannel spectrometer (Fastevert S-2400, Soma Optics Ltd.) equipped with a quartz immersion probe for low temperatures (Hellma, 661-202-UV). Magnetic susceptibility was measured on a Sherwood Scientific MSB-AUTO. Organic products were identified and quantified by a combination of GLC (Shimadzu GC17A (FID equipped with a PHA0201 capillary column and an FID detector (liquid sample) and Hitachi 163 equipped with a Porapak column and an FID detector (gas phase)) and GCMS analyses (Shimadzu QP5000 connected to GC17A equipped with a PHA0201 capillary column). The starting complexes **1^{iPr2}Fe**, **1^{iPr2}Co**, **1^{iPr2}Ni**, and **1$'^{Me3}$Co** were prepared according to the published methods.[27] EHMO calculations were done using the CAChe system (version 4.0). Satisfactory results of the carbon analyses of **4^{Me3}Co**, **6^{iPr2}Fe**, and **8c** were not obtained, despite several attempts, and the best results are shown.

Preparation of 1$'^{Me3}$Fe. To a methanol suspension (50 mL) of $Fe(OAc)_2$ (184 mg, 1.06 mmol) cooled to −78 °C was added a THF solution (50 mL) of $NaTp^{Me3}$ (500 mg, 1.36 mmol) dropwise over 30 min. After removal of the cooling bath the mixture was further stirred for 30 min at ambient temperature. Then the volatiles were removed under reduced pressure and the product was extracted with CH_2Cl_2 (100 mL). Removal of CH_2Cl_2 followed by extraction with MeCN (79 mL), concentration, and cooling to −30 °C gave **1$'^{Me3}$Fe** as a yellow-tan powder (173 mg, 36% yield). **1$'^{Me3}$Fe**: IR (KBr) 2515 (ν_{BH}), 1639 cm^{-1} ($\nu_{C=O}$). Anal. Calcd for $C_{20}H_{31}BN_6O_2Fe$: C, 52.89; H, 6.88; N, 18.50. Found: C, 52.53; H, 6.88; N, 18.19.

Preparation of Hydrocarbyl Complexes. As a typical example, the synthetic procedure for the ethylcobalt complex **6^{iPr2}Co** is described. To a THF solution (5 mL) of **1^{iPr2}Co** (143 mg, 0.26 mmol) cooled to −78 °C was added a THF solution of EtMgBr (1.6 M, 0.21 mL, 0.33 mmol) dropwise. Upon addition the mixture turned from blue to green. After the mixture was warmed to ambient temperature, the volatiles were removed under reduced pressure. The product was extracted with pentane and passed through a Celite plug to remove inorganic salts. Concentration followed by cooling at −30 °C gave **6^{iPr2}Co** (119 mg, 0.22 mmol, 84% yield) as blue cubic crystals. **6^{iPr2}Co**: $\delta_H(C_6D_6)$ 58 (3H), 13 (3H), 5 (18H), −2.0 (18H), −16 (3H). Anal. Calcd for $C_{29}H_{51}N_6BCo$: C, 62.93; H, 9.29; N, 15.18. Found: C, 62.56; 9.52; N, 14.89.

The other hydrocarbyl complexes are prepared following this procedure. The allylnickel (**2^{iPr2}Ni**) and -cobalt (**2^{iPr2}Co**) complexes were crystallized from ether after evaporation of the pentane extracts. The Grignard reagents were prepared in the following solvents: allyl−MgCl/ether; prenyl−MgCl/ether; *p*-methylbenzyl−MgCl/ether; α-naphthylmethyl−MgCl/THF; ethyl−MgBr/THF. The intense Me signals of the $Tp^{R'}$ ligands (^{1}H NMR) for paramagnetic compounds are indicated as "Me", but only intensities are noted for other signals. Other spectral data for the cobalt and iron complexes are summarized in Table 3.

2^{iPr2}Ni: ^{1}H NMR (C_6D_6, room temperature) δ_H 6.10−5.85 (1H, m, allyl CH), 5.94 (3H, s, 4-pz H), 3.59 (3H, sept, J = 7 Hz, C*H*Me$_2$), 3.23 (2H, d, J = 7 Hz, *syn*-allyl CH_2), 3.05 (3H, sept, J = 7 Hz, C*H*Me$_2$), 2.42 (2H, d, J = 12 Hz, *anti*-allyl CH_2), 1.23 (18H, d, J = 6.8 Hz, CH*Me*$_2$), 1.20 (18H, d, J = 7 Hz, CH*Me*$_2$); ^{13}C NMR (C_6D_6, room temperature) δ_C 160.6, 156.0 (s *x* 2, 3- or 5-pz), 102.3 (d, J = 160 Hz, allyl CH), 98.0 (d, J = 170 Hz, 4-pz), 47.7 (t, J = 160 Hz, allyl-CH_2), 28.4, 26.7 (d, J = 125 Hz, *C*HMe$_2$), 23.8, 23.7 (q × 2, J = 125 Hz, CH*Me*$_2$). IR (ν_{B-H}): 2531 (KBr), 2471 cm^{-1} (hexane solution). Anal. Calcd for $C_{30}H_{51}N_6BNi$: C, 63.74; H, 9.09; N, 14.87. Found: C, 63.74; 9.09; N, 14.84.

2^{iPr2}Co: ^{1}H NMR (C_6D_6) δ_H 2.2 (18H, Me), 20 (3H), 6.4 (3H), 0 (3H), −2.3 (18H, Me). Anal. Calcd for $C_{30}H_{51}N_6BCo$: C, 63.72; H, 9.09; N, 14.86. Found: C, 61.66; H, 8.78; N, 14.88.

2^{iPr2}Fe: ^{1}H NMR (C_6D_6) δ_H 72.9 (BH), 52.8 (3H), 43.8 (3H), 14.7 (18H, Me), −24.3 (18H, Me), −78.0 (3H). Anal. Calcd for $C_{30}H_{51}N_6BFe$: C, 64.07; H, 9.14; N, 14.94. Found: C, 63.66; H, 9.07; N, 14.92.

3^{iPr2}Ni: ^{1}H NMR (C_6D_6, room temperature) δ_H 5.98 (3H, s, 4-pz H), 4.42 (1H, t, J = 11 Hz, CH), 3.1−3.2 (6H, br, C*H*Me$_2$), 2.14 (2H, br, CH_2), 1.36, 1.12 (18H × 2, d × 2, J = 7 Hz, CH*Me*$_2$), 0.84, 0.75 (3H × 2, s × 2, Me in prenyl); ^{1}H NMR (C_6D_6, 70 °C) δ_H 5.95 (3H, s, 4-pz H), 4.52 (1H, t, J = 11 Hz, CH), 3.1−3.25 (6H, br, C*H*Me$_2$), 2.3 (2H, br, CH_2), 1.35, 1.18 (18H × 2, d × 2, J = 7 Hz, CH*Me*$_2$), 0.82, 0.77 (3H × 2, s × 2, Me in prenyl); ^{1}H NMR (CD_2Cl_2, −30 °C) δ_H 5.94 (1H, s, 4-pz H), 5.81 (2H, s, 4-pz H), 4.0−4.1 (1H, m, CH), 3.42 (2H, br, C*H*Me$_2$), 3.26 (1H, br, C*H*Me$_2$), 3.05 (2H, br, C*H*Me$_2$), 2.86 (1H, br, C*H*Me$_2$), 2.54 (1H, d, J = 13 Hz, =CH_2), 1.86 (1H, d, J = 9 Hz, =CH_2), 1.0−1.5 (36H, m, CH*Me*$_2$), 0.83, 0.67 (3H × 2, s × 2, Me in prenyl); IR (ν_{B-H}) 2531 (KBr), 2471 cm^{-1} (hexane solution). An analytically pure sample could not be obtained.

4^{iPr2}Fe: ^{1}H NMR (C_6D_6) δ_H 76 (1H), 68 (3H), 52 (3H), 45 (3H), 39 (2H), 15 (18H), −2.9 (2H), −25 (18H), −83.6 (3H). Anal. Calcd for $C_{29}H_{55}N_6BFe$: C, 67.10; H, 8.85; N, 13.41. Found: C, 66.75; H,8.61; N, 13.37.

4^{iPr2}Co: ^{1}H NMR (C_6D_6) δ_H 82.3 (3H), 59.7 (3H), 32.3 (2H), 13.0 (3H), 4.9 (18H, Me), −1.8 (18H, Me), −15.3 (3H), −67.0 (2H). Anal. Calcd for $C_{29}H_{55}N_6BCo$: C, 66.77; H, 8.80; N, 13.35. Found: C, 67.08; H, 8.96; N, 13.50.

(27) **1^{iPr2}Fe**: Ito, M.; Amagai, H.; Fukui, H.; Kitajima, N.; Moro-oka, Y. *Bull. Chem. Soc. Jpn.* **1996**, *69*, 1937. **1^{iPr2}Co,Ni**: Kitajima, N.; Hikichi, S.; Tanaka, M.; Moro-oka, Y. *J. Am. Chem. Soc.* **1993**, *115*, 5496. **1$'^{Me3}$Co**: Submitted for publication.

5^{iPr2}Co: ^{1}H NMR (C_6D_6) δ_H 61.0 (3H), 36.0 (3H), 33 (1H), 18.3 (1H), 13.0 (3H), 4.7 (18H, Me), −6.9 (1H), −11.1 (1H), −1.7 (18H, Me), −14.7 (1H), -87.5 (1H), −99.2 (1H). Anal. Calcd for $C_{38}H_{55}N_6BCo$: C, 68.57; H, 8.33; N, 12.63. Found: C, 68.06; H, 8.41; N, 12.93.

4^{Me3}Co: ^{1}H NMR (C_6D_6) δ_H 81.7 (3H), 32.3 (2H), 17.2 (9H, Me), 11.9 (9H, Me), 4.2 (9H, Me), −65.9 (2H). Anal. Calcd for $C_{26}H_{37}N_6BCo$: C, 62.04; H, 7.41; N, 16.07. Found: C, 61.42; H,7.32; N, 16.73.

6^{iPr2}Fe: ^{1}H NMR (C_6D_6) δ_H 89.3 (BH), 49.6 (6H), 17.0 (18H, Me), −30.9 (18H, Me), −97.9 (3H). Anal. Calcd for $C_{29}H_{51}N_6BFe$: C, 63.28; H, 9.34; N, 15.27. Found: C, 61.90; N, 9.03; N, 15.56.

6^{iPr2}Co: ^{1}H NMR (C_6D_6) δ_H 58 (3H), 13 (3H), 5 (18H, Me), −2.0 (18H, Me), −16 (3H).

Thermolysis of Ethyl Complexes 6^{iPr2}. A heptane solution (10 mL) of **6^{iPr2}** (ca. 0.18 mmol) was placed in an Ar-flushed glass autoclave (50 mL) with a silicone rubber septum. After addition of an appropriate amount of propane (internal standard) through the rubber septum, the mixture was heated in an oil bath at an appropriate temperature. A sample was occasionally taken with a microsyringe through the rubber septum, and the product was analyzed by GLC.

Protonation of Hydrocarbyl Complexes. Toluene solutions (5 mL) of **2**, **4**, and **6** (ca. 0.18 mmol) were treated with aqueous HCl solution (3 M, 1 mL). Then the mixture was stirred for 30 min at room temperature, and the product was analyzed by GLC after addition of appropriate internal standards (ethane (gas phase), propane; *p*-xylene (solution phase), decane).

Hydrogenation of Hydrocarbyl Complexes. Toluene solutions (5 mL) of **2**, **4**, and **6** (ca. 0.18 mmol) were stirred under an H_2 atmosphere in a glass autoclave. Quantification of gases (propene and ethane) was carried out after addition of an internal standard, and that of *p*-xylene was done after trap-to-trap distillation under reduced pressure.

Carbonylation of Hydrocarbyl Complexes. (i) Carbonylation of Iron Complexes. As a typical example, the procedure for the (*p*-methylbenzyl)iron complex **4^{iPr2}Fe** is described. An ethereal solution (5 mL) of **4^{iPr2}Fe** (150 mg, 0.24 mmol) was cooled to −78 °C, and the flask was evacuated and filled with CO. The resultant mixture was warmed to room temperature and stirred for 30 min. After removal of the volatiles under reduced pressure, the residue was washed with hexane (2 mL) to leave yellow **7b** (92 mg, 0.13 mmol, 54% yield). **7b**: ^{1}H NMR (CD_2Cl_2, room temperature) δ_H 7.34, 7.03 (2H × 2, d × 2, J = 7.8 Hz, C_6H_4), 5.97 (1H, s, 4-pz H), 5.94 (2H, s, 4-pz H), 4.54 (2H, s, CO−CH_2), 3.97 (1H, sept, J = 6.7 Hz, C*H*Me_2), 3.45 (3H, sept, J = 6.7 Hz, C*H*Me_2), 2.96 (3H, sept, J = 6.7 Hz, C*H*Me_2), 2.13 (3H, s, *p*-Me), 1.37−1.06 (36H, m, CH*Me*$_2$); ^{13}C NMR (CD_2Cl_2, room temperature) δ_C 255.7 (s, C═O), 215.0 (s, CO), 163.1, 162.5, 156.3, 155.8 (s × 4, 3- or 5-pz), 135.9, 132.9 (s × 2, *ipso*- or *p*-C_6H_4), 129.8, 128.8 (d × 2, J = 154 Hz, *o*- or *m*-C_6H_4), 99.7, 99.0 (d × 2, J = 175 Hz, 4-pz), 68.9 (t, J = 135 Hz, CH_2), 37.4 (q, J = 132 Hz, *p*-Me), 29.6, 29.1, 26.3, 24.0 (d × 4, J = 126 Hz, *C*HMe_2), 26.5, 24.2, 23.6, 23.5, 23.2, 22.8 (q × 6, J = 130 Hz, CH*Me*$_2$); IR (KBr): 2535 (ν_{BH}), 2019, 1952 ($\nu_{C\equiv O}$), 1673 cm^{-1} ($\nu_{C=O}$); IR (hexane) 2540 (ν_{BH}), 2017, 1954 ($\nu_{C\equiv O}$), 1671 cm^{-1} ($\nu_{C=O}$). Anal. Calcd for $C_{38}H_{55}O_3N_6Fe$: C, 64.23; H, 7.80; N, 11.83. Found: C, 64.01; H, 7.92; N, 11.94.

Because the (hydrocarbyl)iron complexes were very sensitive, they could be carbonylated without isolation. Carbonylation of the pentane extracts (the filtrate through a Celite plug) obtained from the reaction of **1Fe** with appropriate Grignard reagents gave the acyl complexes **7**. Complexes **7c** (62% yield) and **7d** (63%) were prepared by this method, but **7a** could not be isolated in a pure form due to contamination with paramagnetic impurities and characterized on the basis of the IR data similar to **7c**,**d**. Essentially the same results were obtained by the Grignard reaction under a CO atmosphere.

7a: IR (KBr) 2522 (ν_{BH}), 2028, 2004, 1964, 1939 ($\nu_{C\equiv O}$), 1666, 1622 cm^{-1} ($\nu_{C=O}$).

7c: ^{1}H NMR (CD_2Cl_2, room temperature) δ_H 6.39 (2H, s, 4-pz H), 6.36 (1H, s, 4-pz H), 4.30 (1H, sept, J = 6.8 Hz, C*H*Me_2), 3.90 (2H, sept, J = 6.8 Hz, C*H*Me_2), 3.89 (1H, sept, J = 6.8 Hz, C*H*Me_2), 3.67 (2H, q, J = 7.0 Hz, CH_2CH_3), 1.33, 1.25, 1.11, 1.09 (6H × 4, d, J = 6.8 Hz, CH*Me*$_2$) (the methyl signal of the propanoyl ligand is overlapped with those of the bristling isopropyl methyl signals); ^{13}C NMR (CD_2Cl_2, room temperature) δ_C 259.5 (C═O), 215.0 (CO), 163.0, 162.6, 156.3, 155.8 (s × 4, 3,5-pz), 99.7, 98.9 (s × 2, 4-pz), 56.8 (t, J = 130 Hz, CH_2), 29.6, 29.0, 26.6, 26.3 (d × 4, J = 126 Hz, *C*HMe_2), 23.6, 23.3 (q × 2, J = 130 Hz, CH*Me*$_2$), 11.1 (q, J = 127 Hz, CH_2CH_3); IR (KBr) 2553 (ν_{BH}), 2024, 2000, 1957, 1930 ($\nu_{C\equiv O}$), 1668, 1620 cm^{-1} ($\nu_{C=O}$); IR (hexane) 2539 (ν_{BH}), 2029, 2015, 1968, 1951 ($\nu_{C\equiv O}$), 1669, 1616 ($\nu_{C=O}$) cm^{-1}. Anal. Calcd for $C_{32}H_{51}O_3N_6Fe$: C, 60.58; H, 8.10; N, 13.25. Found: C, 60.57; H, 8.31; N, 13.23.

7d (a mixture of almost equimolar amounts of two isomers): ^{1}H NMR (CD_2Cl_2 −70 °C) δ_H 7.12, 7.02, 6.99, 6.68 (2H *x* 4, d *x* 4, J = 7.6 Hz, C_6H_4), 4.59, 3.48 (2H, s, CH_2), Me signals (s): 2.49 (3H), 2.37 (6H), 2.29 (3H), 2.24 (6H), 2.23 (6H), 2.22 (3H), 2.21 (3H), 2.20 (6H), 2.00 (6H), 1.92 (6H), 1.85 (3H), 1.81 (3H), 1.79 (6H). ^{13}C NMR (CD_2Cl_2, −70 °C) δ_C 268.8, 258.9 (C═O), 214.3, 211.7 (CO), 150.1, 149.8, 149.3, 142.5, 141.8, 141.5 (3,5-pz), 135.9, 135.3, 133.1, 133.0 (s *x* 4, *ipso*- and *p*-C_6H_4), 129.4, 129.2, 128.8, 128.2 (d, J = 157 Hz, *o*- and *m*-C_6H_4), 113.5, 113.0, 112.6, 112.3 (s *x* 4, 4-pz), 69.6, 58.8 (t, J = 128 Hz, CH_2), 20.9, 20.8, 13.7, 13.5, 12.4, 12.1, 10.9, 10.8, 10.3, 8.1, 8.0, 7.9 (q *x* 12, J = 130 Hz, Me groups in pz^{Me3} and C_6H_4Me). IR (KBr) 2521 (ν_{BH}), 2026, 1964 ($\nu_{C\equiv O}$), 1631 cm^{-1} ($\nu_{C=O}$), (hexane) 2538 (ν_{BH}), 2031, 1968 ($\nu_{C\equiv O}$), 1628 cm^{-1} ($\nu_{C=O}$). Anal. Calcd for $C_{29}H_{37}O_3N_6BFe$: C, 59.61; H, 6.38; N, 14.38. Found: C, 59.44; H, 6.50; N, 14.68.

(ii) Carbonylation of Cobalt Complexes. The cobalt complexes **8c**,**e** were prepared by following the procedure described for the iron complexes. **8c**: Anal. Calcd for $C_{31}H_{51}O_2N_6BCo$: C, 61.09; H, 8.43; N, 13.79. Found: C, 60.20; H, 8.43; N, 13.76. An analytically pure sample of **8e** was not obtained, despite several attempts.

(iii) Preparation of Propanoylnickel Complex 10. To a THF solution (7 mL) of **1^{iPr2}Ni** (145 mg, 0.26 mmol) cooled to −78 °C was added a THF solution of EtMgBr (1.5 M, 0.26 mL, 0.39 mmol). Upon addition of the Grignard reagent the color changed from pink to green. After the Schlenk tube was evacuated, CO was refilled and the mixture was gradually warmed to room temperature and stirred for 30 min. CO replacement caused an immediate color change to orange. Then the volatiles were removed under reduced pressure and the product was extracted with pentane (50 mL) and passed through a Celite plug. The pentane extract was evaporated, and the resulting residue was crystallized from ether to give **10** (112 mg, 0.81 mmol, 71% yield) as orange cubic crystals. **10**: ^{1}H NMR (CD_2Cl_2, room temperature) δ_H 5.84 (3H, s, 4-pz H), 3.44, 3.15 (3H × 2, sept, J = 6.8 Hz, C*H*Me_2), 1.88 (2H, q, J = 7.4 Hz, CH_2CH_3), 1.22, 1.20 (18H × 2, d × 2, J = 6.84 Hz, CH*Me*$_2$), 0.45 (3H, t, J = 7.4 Hz, CH_2CH_3); ^{13}C NMR (CD_2Cl_2, room temperature) δ_C 225.9 (C═O), 187.4 (CO), 160.3, 156.3 (3,5-pz), 98.0 (d, J = 179 Hz, 4-pz), 40.7 (t, J = 132 Hz, CH_2), 28.2, 26.6, 23.6, 23.3 (q × 4, J = 128 Hz, CH*Me*$_2$), 11.1 (q, J = 127 Hz, CH_2CH_3); IR (KBr): 2547 (ν_{BH}), 2009 ($\nu_{C\equiv O}$), 1685 cm^{-1} ($\nu_{C=O}$). Anal. Calcd for $C_{31}H_{51}O_2N_6BNi$: C, 61.11; H, 8.44; N, 13.79. Found: C, 60.89; H, 8.26; N, 13.93.

Oxygenation of Hydrocarbyl Complexes. Toluene solutions (5 mL) of **2**, **4**, and **6** (ca. 0.18 mmol) placed in a Schlenk tube was cooled to −78 °C, evacuated, and refilled with O_2. Then the mixture was warmed to room temperature and the

products were analyzed by GLC after addition of appropriate internal standards.

Reaction with Organic Substrates. A toluene solution (5 mL) containing **6^{iPr2}** (0.18 mmol) and an appropriate organic substrate (0.18 mmol) was heated for 30 min at 70 °C in an oil bath. After the mixture was cooled to room temperature, aqueous HCl solution (3M, 1,9 mL) and an appropriate internal standard were added and the organic phase was subjected to GLC analysis. An authentic sample of 1-phenyl-1-butene was prepared according to the literature procedure.[28]

Reaction of 6^{iPr2}Fe with Phenylacetylene Followed by Carbonylation. An ethereal solution of **6^{iPr2}Fe** (197 mg, 0.36 mmol) and PhC≡CH (60 mL, 0.54 mmol) was stirred for 4 h at 35 °C, and the color of the mixture changed to pale green-yellow. Then the Schlenk tube was cooled to −78 °C, evacuated, and refilled with CO. The resultant mixture was stirred for 30 min at ambient temperature. After removal of the volatiles under reduced pressure the residue was crystallized from ether to give **12** (142 mg, 0.21 mmol), 58% yield) as yellow crystals. **12**: ^{1}H NMR (C_6D_6, room temperature) δ_H 7.51 (2H, d, J = 6.3 Hz *o*-Ph), 7.09−6.89 (3H, m, *m*- and *p*-Ph), 6.04 (2H, s, 4-pz H), 5.90 (1H, s, 4-pz H), 4.77 (2H, sep, J = 6 Hz, C*H*Me$_2$), 3.60−3.39 (4H, m, C*H*Me$_2$), 1.43−1.07 (36H, m, CH*Me*$_2$); ^{13}C NMR (CD_2Cl_2, room temperature) δ_C 213.0 (s, CO), 165.5, 164.0, 157.2, 156.7 (s × 4, 3 or 5-pz), 131.4 (d, J = 160 Hz, *o*-, or *m*-Ph), 128.7(s, *ipso*-Ph), 131.4 (d, J = 150 Hz, *o*- or *m*-Ph), 125.3 (d, J = 160 Hz, *p*-Ph), 117.2, 100.9 (s × 2, C≡C), 100.4, 99.7 (d × 2, J = 170 Hz, 4-pz), 31.9, 29.6, 28.5, 26.6 (d × 4, J = 126 Hz, *C*HMe$_2$), 26.5, 24.6, 24.4, 24.1, 23.5, 23.4 (q × 6, J = 132 Hz, CH*Me*$_2$); IR (KBr) 2545 (ν_{BH}), 2108 ($\nu_{C\equiv C}$), 2043, 1991 cm^{-1} ($\nu_{C\equiv O}$). Anal. Calcd for $C_{37}H_{51}O_2N_6$-BFe: C, 65.50; H, 7.58; N, 12.39. Found: C, 66.02; H, 8.52; N, 11.36.

X-ray Crystallography. Diffraction measurements were made on a Rigaku RAXIS IV imaging plate area detector with Mo Kα radiation (λ = 0.710 69 Å). All the data collections were carried out at −60 °C. Indexing was performed from 3 oscillation images which were exposed for 4 min. The crystal-to-detector distances were 100 mm (**2^{iPr2}Ni,Co**) and 110 mm (**2^{iPr2}Fe**, **4^{iPr2}Fe**). Data collection parameters were as follows (oscillation range/number of oscillation images/exposure time): 4.5°/33/60 min (**2^{iPr2}Ni**), 6°/22/60 min (**2^{iPr2}Co**), 3°/29/45 min (**2^{iPr2}Fe**), 5°/ 33/90 min (**4^{iPr2}Fe**), 4°/20/80 min (**6^{iPr2}Co**), 5°/ 16/75 min (**10**). Readout was performed with a pixel size of 100 μm × 100 μm.

Crystallographic data and the results of refinements are summarized in Table 5. The structural analysis was performed on an IRIS O2 computer using the teXsan structure solving program system[29] obtained from the Rigaku Corp., Tokyo, Japan. Neutral scattering factors were obtained from the standard source.[30] In the reduction of data, Lorentz and polarization corrections were made. An absorption correction was also made.[31]

The structures were solved by a combination of direct methods (SHELXS-86[32] or SAPI91 or SIR92 or MITHRIL90)[33]

Table 5. Crystallographic Data

	1^{iPr2}Ni	**2^{iPr2}Ni**	**2^{iPr2}Co**	**2^{iPr2}Fe**	**3^{iPr2}Ni**	**4^{iPr2}Fe**	**4^{Me3}Co**	**5^{iPr2}Co**	**6^{iPr2}Co**	**10**
formula	$C_{27}H_{46}BN_6ClNi$	$C_{30}H_{51}BN_6Ni$	$C_{30}H_{51}BN_6Co$	$C_{30}H_{51}BN_6Fe$	$C_{32}H_{55}BN_6Ni$	$C_{35}H_{55}BN_6Fe$	$C_{26}H_{37}BN_6Co$	$C_{38}H_{55}BN_6Co$	$C_{26}H_{51}BN_6Co$	$C_{31}H_{51}BN_6O_2N$
fw	559.7	565.3	565.5	562.4	593.3	626.5	503.4	665.6	553.5	609.3
cryst syst	monoclinic	triclinic	triclinic	orthorhombic	monoclinic	triclinic	triclinic	monoclinic	monoclinic	monoclinic
space group	$P2_1/m$	$P\bar{1}$	$P\bar{1}$	$P2_12_12_1$	$P2_1/n$	$P\bar{1}$	$P\bar{1}$	$P2_1/n$	$P2_1/c$	$P2_1/n$
a/Å	9.995(3)	9.778(3)	9.733(8)	18.796(2)	18.361(2)	11.818(9)	11.337(5)	12.531(9)	10.309(3)	9.968(5)
b/Å	16.243(4)	16.76(1)	16.818(8)	16.319(2)	17.987(5)	16.39(1)	13.274(2)	11.981(2)	16.206(17)	15.820(2)
c/Å	19.098(6)	9.720(8)	9.718(9)	21.653(4)	10.813(1)	9.408(4)	10.7164(15)	25.780(6)	19.207(5)	21.570(2)
α/deg		91.438(4)	90.88(6)			90.56(4)	104.819(11)			
β/deg	102.01(2)	102.87(7)	101.59(5)		99.969(9)	101.29(4)	104.30(3)	102.18(3)	100.02(2)	97.02(2)
γ/deg		90.96(7)	92.20(5)			91.46(5)	110.749(3)			
V/Å^3	3033(2)	1552(1)	1557(2)	6642(1)	3517.3(9)	1786(2)	1352.5(7)	3783(3)	3160(4)	3376(2)
Z	4	2	2	8	4	2	2	4	4	4
d_{calcd}/g·cm^{-3}	1.23	1.21	1.21	1.13	1.12	1.17	1.24	1.17	1.16	1.20
μ/cm^{-1}	7.53	6.54	5.80	4.80	5.80	4.53	6.6	4.9	5.7	6.1
2θ/deg	up to 50	up to 50	up to 50	up to 53.6	up to 55.1	up to 54.4	up to 50	up to 50	up to 55	up to 50
no. of data collected	4754	4249	4432	6702	7276	5141	4472	5092	4201	5171
no. of unique data with $F > 4\sigma(F)$	4090	3918	4217	6058	6797	3809	3997	4949	3267	4955
no. of params refined	337	355	355	709	375	401	317	438	347	432
R1[a]	0.073	0.083	0.072	0.076	0.053	0.104	0.074	0.086	0.083	0.064
wR2[b]	0.203	0.218	0.197	0.218	0.153	0.273	0.192	0.225	0.224	0.182

[a] R1 = $[\sum||F_o| - |F_c||]/\sum|F_o|$ (for data with $F > 4\sigma(F)$). [b] wR2 = $[\sum\{w(F_o^2 - F_c^2)\}^2/\sum\{w(F_o^2)^2\}]^{0.5}$; $w = 1/[\sigma^2(F_o^2) + (0.1000P)^2]$ where $P = [2F_c^2 + \mathrm{Max}(F_o^2,0)]/3$ (for all data).

(28) Buddrus, J. *Chem. Ber.* **1964**, *107*, 2050.

(29) teXsan: Crystal Structure Analysis Package, version 1.11; Rigaku Corp., Tokyo, Japan, 2000.

(30) *International Tables for X-ray Crystallography*; Kynoch Press: Birmingham, U.K., 1975; Vol. 4.

(31) Higashi, T. Shape—Program To Obtain Crystal Shape using CCD Camera; Rigaku Corp.: Tokyo, Japan, 1999.

(32) (a) Sheldrick, G. M. SHELXS-86: Program for Crystal Structure Determination; University of Göttingen, Göttingen, Germany, 1986. (b) Sheldrick, G. M. SHELXL-97: Program for Crystal Structure Refinement; University of Göttingen, Göttingen, Germany, 1997.

(33) (a) SAPI91: Fan, H.-F. Structure Analysis Programs with Intelligent Control, Rigaku Corp., Tokyo, Japan, 1991. (b) SIR92: Altomare, A.; Burla, M. C.; Camalli, M.; Cascarano, M.; Giacovazzo, C.; Guagliardi, A.; Polidori, G. *J. Appl. Crystallogr.* **1994**, *27*, 435. (c) MITHRIL90: Gilmore, C. J. MITHRIL—An Integrated Direct Methods Computer Program; University of Glasgow: Glasgow, U.K., 1990.

and Fourier synthesis (DIRDIF94).[34] Least-squares refinements were carried out using SHELXL97[32] (refined on F^2) linked to teXsan. All the non-hydrogen atoms were refined anisotropically. Riding refinements were applied to the methyl hydrogen atoms of the isopropyl groups (B(H) = B(C)), and the other hydrogen atoms were fixed at the calculated positions. The absolute configuration of **2^{iPr2}Fe** of the centrosymmetric space group was determined by comparison of the magnitudes of the R value and the Flack parameter with those of the other enantiomers. Details of the refinements of **10** are as follows. It was found that a part of the isopropyl methyl groups was disordered and two components were considered (C25−26:C25a−C26a = 0.512:0.488; C28−29:C28a−C29a = 0.565:0.435; C38−C39:C38a−C39a = 0.577:0.423). Riding refinements were applied to the methyl hydrogen atoms (B(H) = B(C)) except for the disordered part, and the other hydrogen atoms except for the methine hydrogen atoms in the disordered isopropyl groups were located at the calculated positions and not refined. The hydrogen atoms involved in the disordered parts were not included in the refinement.

(34) Beurskens, P. T.; Admiraal, G.; Beurskens, G.; Bosman, W. P.; Garcia-Granda, S.; Gould, R. O.; Smits, J. M. M.; Smykalla, C. The DIRDIF Program System; Technical Report of the Crystallography Laboratory; University of Nijmegen, Nijmegen, The Netherlands, 1992.

Acknowledgment. We are grateful to the Ministry of Education, Culture, Sports, Science, and Technology of the Japanese Government for financial support of this research (Grants-in-Aid for Scientific Research: 08102006 and 11228201). N.S. is grateful to the Japan Society of Promotion of Science for the support, and T.T.N. was a visiting scholar of the International Course for Advanced Research in Chemistry and Chemical Engineering sponsored by UNESCO and the Ministry of Education, Culture, Sports, Science and Technology of the Japanese Government. We also thank the Mitsubishi Chemical Co. for evaluation of the catalytic activity of **1^{iPr2}Fe,Co** for ethylene polymerization and Dr. Masato Oshima (Tokyo Institute of Technology) for preliminary DFT calculation on **4^{Me3}Co**.

Supporting Information Available: EHMO diagrams for Me−Co(CO)$_4$ and Tp^{M}Fe−Me and atomic numbering schemes and tables of positional parameters, anisotropic thermal parameters, and bond lengths and angles. This material is available free of charge via the Internet at http://pubs.acs.org.

OM0103106